

Enhancing the Tensor Normal via Geometrically Parameterized Cholesky Factors

Quinn Simonis and Martin T. Wells *

Cornell University

April 2025

Abstract

In this article, we explore Bayesian extensions of the tensor normal model through a geometric expansion of the multi-way covariance's Cholesky factor inspired by the Fréchet mean under the log-Cholesky metric. Specifically, within a tensor normal framework, we identify three structural components in the covariance of the vectorized data. By parameterizing vector normal covariances through such a Cholesky factor representation, analogous to a finite average of multiway Cholesky factors, we eliminate one of these structural components without compromising the analytical tractability of the likelihood, in which the multiway covariance is a special case. Furthermore, we demonstrate that a specific class of structured Cholesky factors can be precisely represented under this parameterization, serving as an analogue to the Pitsianis-Van Loan decomposition. We apply this model using Hamiltonian Monte Carlo in a fixed-mean setting for two-way covariance relevancy detection of components, where efficient analytical gradient updates are available, as well as in a seasonally-varying covariance process regime.

Keywords: Bayesian models, covariances estimation, Fréchet mean, Hamiltonian Monte Carlo, Log-Cholesky metric, Geodesic Monte Carlo, multiway models, Kronecker product,

*Department of Statistics and Data Science, Cornell University; qas3@cornell.edu, mtw1@cornell.edu

Introduction

This article explores the generalization of a classical likelihood function for multimodal data, where observations are represented as tensors $\mathcal{Y} \in \mathbb{R}^{\times_{i=1}^D d_i}$. The normal tensor model assumes Gaussianity in each mode, which means that individual elements follow $y_{i_1, i_2, \dots, i_D} \sim \mathcal{N}(0, 1)$. Mode-wise products enable the construction of a broad class of distributions that capture correlations along specific modes. Alternatively, tensor normal models can be viewed through the lens of vectorization. Assuming lexicographic order, if $\mathcal{Y} \sim \mathcal{TN}(M, \{\Sigma_i\}_{i=1}^D)$, then its vectorized form follows $\text{vec}(Y) \sim \mathcal{N}(\text{vec}(M), \otimes_{i=D}^1 \Sigma_i)$.

This likelihood is particularly valuable in Bayesian analysis for examining correlations in high-dimensional data, as it naturally decomposes complex dependencies into lower-dimensional components. Applications of the tensor normal model include analysis of mortality data [8], assessment of healthcare [15], and modeling in space time [5, 11]. Beyond the two-way case, higher-order examples arise in relational data analysis [18], where a Bayesian approach extends the tensor normal model through the Tucker product.

Although the tensor normal model offers computational advantages, it imposes structural assumptions on global covariance that may not accurately capture the underlying data-generating process [3, 29].

Our work is closely aligned with the literature on Kronecker product expansions of covariances. This area of work was inspired by the work of [26], where the authors show that in fact any arbitrary matrix $Q \in \mathbb{R}^{d_1 d_2 \times d_1 d_2}$ can be represented as:

$$Q = \sum_{i=1}^{r^2} A_i \otimes B_i, \quad A_i \in \mathbb{R}^{d_1 \times d_1}, \quad B_i \in \mathbb{R}^{d_2 \times d_2}, \quad r = \min\{d_1, d_2\}.$$

Literature in Kronecker product expansions of covariances has attracted attention within a statistical context, wherein the goal is often to find a minimal d to adequately represent a covariance matrix as a sum of Kronecker products:

$$\Sigma \approx \sum_{i=1}^d A_i \otimes B_i, \quad A_i \in \mathcal{P}^+(d_1), B \in \mathcal{P}^+(d_2), \quad (1)$$

where $\mathcal{P}^+(d)$ denotes the manifold of $d \times d$ symmetric positive definite (SPD) matrices. Examples

include [30], who investigated using Kronecker product expansions to model matrix-valued data using a penalized least squares approach.

In this article, we develop a Bayesian model selection procedure to identify the level of structural sparsity in the strictly lower triangular entries of the Cholesky factor for a multiway covariance. This approach leverages a geometrically inspired parametrization of Cholesky factors for multiway covariances, addressing one of the key structural assumptions imposed by the tensor normal model.

Our work is motivated by the log-Cholesky metric [23], which observes that Cholesky factors of symmetric positive definite (SPD) matrices form a topological manifold, wherein the author endows this manifold with a Riemannian metric that has a closed form Fréchet mean. Building on this, we express the Cholesky factor of an arbitrary SPD matrix of Cholesky factors of multiway SPD matrices, introducing a simplex-distributed random variable to regulate the structural complexity of lower triangular entries. This alternative parametrization maintains full analytic expressivity, and we employ Hamiltonian Monte Carlo [25] to avoid the constraints of conditional conjugacy required by Gibbs sampling.

The remainder of the paper is structured as follows:

- Section 1 provides the mathematical background of the paper, with an introduction to Hamiltonian Monte Carlo in Section 1.1, and the Tensor Normal distribution, and its structural limitations in Section 1.2.
- Section 2 introduces the differential geometry of Cholesky factors in Section 2.1 used to extend the multiway covariance parameterization of the tensor normal in Section 2.2. The latter subsection also provides bounds on approximation quality of arbitrary Cholesky factors of symmetric positive definite matrices under our parameterization.
- Section 3 provides auxiliary results for centering matrix priors in section 3.1, and two Bayesian models are proposed in Sections 3.2 and 3.3 for static and seasonally dynamic covariance implementations, respectively.
- Section 4 provide results detailing our choice in the use of `stan` as our sampling algorithm over a Geodesic Monte Carlo implementation.
- Section 5 provides simulated data examples for assessing the quality of the model’s ability

to adequately recognize degree of separability for a data generating processes’ covariance in static and seasonally dynamic covariances in Sections 5.1 and 5.2, respectively.

- Section 6 provides real data applications of our model in a static case to the Wisconsin Breast Cancer dataset in Section 6.1 and a dynamic implementation for the analysis of coefficients in a Bayesian regression of continental US climate data corresponding to annual cyclic patterns in Section 6.2.
- Section 7 provides potential future directions of work, and Section 8 provide supplementary details for efficient Hamiltonian Monte Carlo implementation of the static and seasonally dynamic parameterizations in Sections 8.1 and 8.2, respectively.

1 Mathematical Background

1.1 Bayesian Inference

Bayesian inference aims to characterize the latent structure of a parameter space Γ given a collection of observations $Y = \{y_1, \dots, y_n\}$. We do so assuming a prior distribution in our parameter space $p(\Gamma)$ and the likelihood of our data parameterized by $L(y; \Gamma)$. The goal of Bayesian inference is to characterize the posterior distribution of Γ given Y according to Bayes theorem

$$P(\Gamma|Y) = \frac{L(Y; \Gamma)P(\Gamma)}{\int_{\gamma} L(Y; \gamma)P(\gamma)d\gamma},$$

however, the calculation of the integral in the denominator is often intractable. As such, posterior inference often resolves to using computational techniques such as MCMC sampling or making approximations with known distributions such as variational inference.

MCMC sampling is asymptotically exact and is generally referred to as the gold standard for computational inference. Historically, MCMC inference is characterized by Gibbs [9] and random walk samplers. Gibbs sampling makes use of sampling from the full conditional posteriors. That is, by sampling from $P(\beta|Y, \Gamma_{-\beta})$. This, however, requires either prior distributions that are conditionally conjugate with the likelihood or analytically tractable expansions that are conditionally conjugate. Often these impose restrictions which limit expressivity of the prior and are difficult to

derive. Random walk samplers, which are not constrained by the necessity of conditional conjugacy, are often slow to draw independent samples from the posterior distribution.

Hamiltonian Monte Carlo [25] is an advanced MCMC technique which extends random walk samplers by leveraging gradient information combined with updates defined by energy-preserving symplectic dynamics [17] to build an ergodic Markov chain, which combined with a Metropolis correction gives asymptotically exact inference.

Mathematically, given a posterior distribution up to normalization, $P^*(q_t|Y) = L(Y; q_t)P(q_t)$, Hamiltonian Monte Carlo works by introducing an auxiliary latent variable p_t with distribution $K(p_t)$, and expressing a tradeoff between p_t and q_t through the time dependent coupled energy preserving differential equations

$$H(q_t, p_t) = P^*(q_t|Y) + K(p_t) \quad (2)$$

$$\frac{\partial q_t}{\partial t} = \frac{\partial H}{\partial p_t} \quad (3)$$

$$\frac{\partial p_t}{\partial t} = -\frac{\partial H}{\partial q_t}. \quad (4)$$

The differential equations (3-4) describe Hamilton's equations of motion. The key point is that under perfect evolution through t , Hamilton's equations give symplectic updates of H . That is, $H(q_t, p_t) = H(q_0, p_0)$. However, practical implementation often does not allow analytic solutions to Hamilton's equations, wherein the resolution is the leapfrog integrator ([20]), where dynamics are discretized as:

$$q_{t+\frac{1}{2}} \rightarrow q_t + \frac{\epsilon}{2} \nabla_{p_t} H(q_t, p_t)$$

$$p_{t+1} \rightarrow p_t + \epsilon \nabla_{q_{t+\frac{1}{2}}} H(q_{t+\frac{1}{2}}, p_t)$$

$$q_{t+1} \rightarrow q_{t+\frac{1}{2}} + \frac{\epsilon}{2} \nabla_{p_{t+1}} H(q_{t+\frac{1}{2}}, p_{t+1})$$

for $t \in \{0, \dots, T\}$. Trajectories under the leapfrog integrator are then accepted according to the Metropolis ratio:

$$\alpha(q_0, q_T) = \min(1, \frac{\exp(-H(q_T, p_T))}{\exp(-H(q_0, p_0))})$$

as $\epsilon \rightarrow 0$, the trajectories converge to symplectic trajectories, yielding a high α potentially at the

cost of high autocorrelation for a choice of T too small. Large choices of ϵ yield trajectories which yield a potentially too small α at the benefit of being highly uncorrelated. The choice of these tuning parameters then often comes down to optimizing based on a apriori choice of α , which for sufficiently uncorrelated samples is typically $\approx .8$ in off the shelf samplers.

1.2 Tensor Normal Distributions

The tensor normal model is a model used in the analysis of multi-indexed Gaussian data. That is, Gaussian data which may itself be reshaped into the form $\mathcal{X} \in \mathbb{R}^{\times_{i=1}^D d_i}$. In particular, construction of the tensor normal class can be understood in terms of the Tucker product [16, 18]: for a tensor $\mathcal{A} \in \mathbb{R}^{\times_{i=1}^D d_i}$, and matrix $B \in \mathbb{R}^{d_i \times d_i}$ the Tucker product is defined as:

$$(\mathcal{A} \times_i B)[k_1, \dots, q_i, \dots, k_D] := \sum_{k_i=1}^{d_i} \mathcal{A}[k_1, \dots, k_i, \dots, k_D] B[k_i, q_i]. \quad (5)$$

Alternatively for a collection of matrices $\mathbf{B} = \{B_1, \dots, B_D\}$, the Tucker product between \mathcal{A} and \mathbf{B} can be stated directly as:

$$(\mathcal{A} \circ \mathbf{B})[q_1, \dots, q_D] := \sum_{k_1=1}^{d_1} \dots \sum_{k_D=1}^{d_D} \mathcal{A}[k_1, \dots, k_D] B_1[k_1, q_1] \dots B_D[k_D, q_D]. \quad (6)$$

The interpretation of this tensor product is that the constituent matrices \mathbf{B} act 'mode-wise' on \mathcal{A} . For example, in the 2-way case:

$$(\mathcal{A} \circ \mathbf{B})[q_1, q_2] := \sum_{k_1=1}^{d_1} \sum_{k_2=1}^{d_2} \mathcal{A}[k_1, k_2] B_1[k_1, q_1] B_2[k_2, q_2] = B_1 \mathcal{A} B_2. \quad (7)$$

A key point of utility in the use of the Tucker product is the ability to compute $(\mathcal{A} \circ \mathbf{B})$ sequentially through:

$$(\mathcal{A} \circ \mathbf{B}) = (((\mathcal{A} \times_1 B_1) \times_2 B_2) \times_3 B_3) \dots \times_i B_i) \times \dots \times_D B_D. \quad (8)$$

To understand the convenience of this operation in terms of the normal distribution, the tensor normal itself is constructed through the assumption that element-wise, \mathcal{A} is standard normal, and

$\mathbf{B}_i \in \mathcal{P}^+(d_i)$, wherein

$$\mathcal{T} \sim TN(\mathcal{M}, \{\Sigma_1, \dots, \Sigma_D\}) \implies T \stackrel{D}{=} \mathcal{A} \circ \{\Sigma_1^{\frac{1}{2}}, \dots, \Sigma_D^{\frac{1}{2}}\} + \mathcal{M}. \quad (9)$$

We can produce an identical construction through the Cholesky factorization by instead letting $\{L_1, \dots, L_D\} = \{\mathcal{L}(\Sigma_1), \dots, \mathcal{L}(\Sigma_D)\}$, where instead:

$$\mathcal{T} \sim TN(\mathcal{M}, \{\Sigma_1, \dots, \Sigma_D\}) \implies T \stackrel{D}{=} \mathcal{A} \circ \{L_1, \dots, L_D\} + \mathcal{M}. \quad (10)$$

Where by [22], we can directly observe the tensor normal distribution is then a special case of the vector normal:

$$\text{vec}(T) \stackrel{D}{=} \otimes_{i=D}^1 L_i \text{vec}(\mathcal{A}) + \text{vec}(\mathcal{M}) \sim N(\text{vec}(\mathcal{M}), \otimes_{i=D}^1 L_i L_i^T) \quad (11)$$

where for $A \in \mathbb{R}^{d_1 \times d_1}$, $B \in \mathbb{R}^{d_2 \times d_2}$, $A \otimes B \in \mathbb{R}^{d_1 d_2 \times d_1 d_2}$ denotes the Kronecker product:

$$A \otimes B = \begin{pmatrix} a_{11}B & \cdots & a_{1,d_1}B \\ \vdots & \ddots & \vdots \\ a_{d_1,1}B & \cdots & a_{d_1,d_1}B \end{pmatrix} \quad (12)$$

however, it's clear that in it's most general form, the vector normal distribution is computationally limited through large matrix multiplications for an arbitrary covariance. Whereas for data which admits a multi-index array structure, greater scalability can be achieved by leveraging the smaller sequential operations from (8) without a significant loss of flexibility as say an assumption of diagonality.

However, it is clear from the Kronecker structured covariance that the tensor normal distribution sacrifices some flexibility for scalability. Recall that the Cholesky decomposition corresponds to a specific choice of conjugate axes for the ellipsoid defined by the set $\{y : y^t(A \otimes B)y = 1\}$. Informally, the shape of this ellipsoid can be characterized by the component-wise eccentricity of the ellipsoid. In other words, the principal axes correspond to the eigenvectors of $A \otimes B$. SVD is known to be

distributed on Kronecker products [31]:

$$A \otimes B = (U_A \otimes U_B)(D_A \otimes D_B)(U_A \otimes U_B).$$

Let $Q = C \oslash D$ denote the Hadamard division between $C, D \in \mathbb{R}^{n \times p}$, which is defined element-wise by:

$$Q_{i,j} = \frac{C_{i,j}}{D_{i,j}}.$$

Then note that

$$(U_A \otimes U_B)[\cdot, d_2(j-1) + i] \oslash (U_A[\cdot, i] \otimes 1_{d_2}) = c_i 1_{d_1 \cdot d_2}$$

where $c_i \in \mathbb{R}$ for all $i, j \in \{1, \dots, d_1\} \times \{1, \dots, d_2\}$. Depending only on the index i , there are then only d_1 distinct principal directions that generate the ellipsoid $y^t(A \otimes B)y = 1$ up to scaling out of the total dimensions $d_1 \cdot d_2$. These repetitions d_2 of each principal direction manifest in the repetitions of duplication and scaling found within the conjugate axes defined by B , scaled by the elements of A . These duplications are only distinct in their scaling, as such the shape as defined by the eccentricity is not distinct in these repetitions.

In Section 2.2, we identify the exact sources of structure present within a Cholesky factorization of a tensor normal covariance and demonstrate that one such source can be completely eliminated without loss of analytic tractability of the likelihood through a simple modification introduced in the next section.

2 Extending the Multiway Parameterization

2.1 Differential Geometry of Cholesky Factors

Let $\mathcal{P}^+(d)$ denote SPD matrices of $d \times d$ full rank, $\mathcal{L}^+(d)$ denote Cholesky factors of $d \times d$ SPD matrices, and $[\mathcal{L}^+](d)$, $\mathbb{D}(\mathcal{L}^+)(d)$ denote correspondingly the spaces of strictly lower triangular and diagonal components of Cholesky factors, respectively. We use $\mathcal{L}(\Sigma)$ to refer to the lower triangular Cholesky factor of Σ , note that $\mathcal{P}^+(d)$ is in bijective correspondence with $\mathcal{L}^+(d)$ and $\Sigma = \mathcal{L}(\Sigma)[\mathcal{L}(\Sigma)]^T$. Let $[\mathcal{L}(\Sigma)]$ and $\mathbb{D}(\mathcal{L}(\Sigma))$ be strictly lower triangular and diagonal entries of $\mathcal{L}(\Sigma)$. If $\mathbf{I} = \{i_1, \dots, i_k\}$ such that $i_j \in \mathbb{N}$, let $\mathcal{P}^+(\mathbf{I})$ denote the set of Kronecker structured

covariance matrices as

$$\mathcal{P}^+(\mathbf{I}) := \{\otimes_{j \in \mathbf{I}} A_j | A_j \in \mathcal{P}^+(i_j)\}$$

and correspondingly the set of Kronecker structured lower triangular Cholesky factors as

$$\mathcal{L}^+(\mathbf{I}) := \{\otimes_{j \in \mathbf{I}} \mathcal{L}(A_j) | \mathcal{L}(A_j) \in \mathcal{L}^+(i_j)\}.$$

A topological manifold is a second countable Hausdorff space which is locally holomorphic to the Euclidean space. For a topological manifold \mathcal{M} , the tangent space at $q \in \mathcal{M}$, $T_q\mathcal{M}$ is defined by the equivalence class of curves parameterized by the space

$$T_q\mathcal{M} := \{\gamma'(0) : \gamma(0) = q\}.$$

By endowing the tangent space of a topological manifold with a continuously varying bi-invariant metric, g , the paired structure (\mathcal{M}, g) then becomes a Riemannian manifold. The key benefit of Riemannian manifolds with regard to this article is that they allow the computation of angles between tangent vectors and thereby allow the construction of distances between points, and importantly the construction of geometrically informed averages on nonlinear spaces, known as Fréchet means.

The Riemannian geometry of the Cholesky factors of the SPD matrices was recently investigated in [23]. In particular, they derive the topological manifold structure of $\mathcal{L}^+(d)$, and endow the space with the following Riemannian metric:

$$g_L(U, V) = \text{tr}(\mathbb{D}(U)\mathbb{D}(L)^{-1}\mathbb{D}(V)\mathbb{D}(L)^{-1}) + \text{tr}([U][V]), \quad U, V \in \mathcal{T}_L\mathcal{L}^+(d).$$

Note that this metric should be viewed as endowed with the diagonal and strictly lower triangular components with a product manifold metric, where the diagonal is equipped with the affine-invariant metric and the strictly lower triangular entries are equipped with the Euclidean metric. For $X \in \mathcal{T}_L\mathcal{L}^+(d)$, the corresponding geodesic at L in the direction of X under this metric are given by:

$$\gamma_{L,X}(t) = [L] + t[X] + \exp(t\mathbb{D}(x)\mathbb{D}(L)^{-1}). \quad (13)$$

For $L_1, L_2 \in \mathcal{L}^+(d)$, the corresponding geodesic distance between L_1 and L_2 is given by:

$$d_{\mathcal{L}^+(d)}(L_1, L_2) = [\|L_1 - L_2\|_F^2 + \|\log \mathbb{D}(L_1) - \log \mathbb{D}(L_2)\|^2]^{\frac{1}{2}}. \quad (14)$$

For a finite sample $\{A_1, \dots, A_n\}$ belonging to a Riemannian manifold (\mathcal{M}, g) with corresponding geodesic distance $d(A, B)$ for $A, B \in \mathcal{M}$, the Fréchet mean over \mathcal{M} is defined as the sum of squares minimization:

$$\mu_g = \arg \min_{x \in \mathcal{M}} \sum_{i=1}^n d^2(x, A_i). \quad (15)$$

Under the log-Cholesky metric, for $\{L_1, \dots, L_n\} \in \mathcal{L}^+(d)$, the corresponding Fréchet mean over $\mathcal{L}^+(d)$ is then given by the quantity

$$\mathbb{E}_n(L_1, \dots, L_n) = \frac{1}{n} \sum_{i=1}^n \lfloor L_i \rfloor + \exp \left\{ \frac{1}{n} \sum_{i=1}^n \log \mathbb{D}(L_i) \right\}. \quad (16)$$

Our first observation is to note that the Fréchet mean of a finite sample of multiway Cholesky factors is, in general, no longer multiway.

Theorem 2.1. *Let L^\dagger be the Cholesky factor such that:*

$$L^\dagger = \sum_{i=1}^n \lfloor \mathcal{L}(A_i) \rfloor + \exp \left\{ \sum_{i=1}^n \log \mathbb{D}(\mathcal{L}(A_i)) \right\} \quad (17)$$

for $A_i \in \mathcal{P}^+(\mathbf{I})$, then $L^\dagger \notin \mathcal{L}^+(\mathbf{I})$, while $\mathbb{D}(L^\dagger) \in \mathbb{D}(\mathcal{L}^+(\mathbf{I}))$.

Proof. For the sake of proof suppose that $L^\dagger \in \mathcal{L}^+(\mathbf{I})$. Then $\exists A, B$ with $A \in \mathbb{D}^+(\mathbf{I})$ and $B \in \lfloor \mathcal{L}^+ \rfloor(\mathbf{I})$ such that $L^\dagger = A + B$. Now note, if $A_i \in \mathcal{P}^+(\mathbf{I})$ for $i \in \{1, \dots, k\}$, then

$$\log \mathbb{D}(\mathcal{L}(A_t)) = \sum_{t=1}^k \otimes_{j=1}^k (1_{j=t} \log(\mathbb{D}(A_t^{(j)})) + 1_{j \neq t} I_j). \quad (18)$$

So we can then write

$$\sum_{i=1}^n \log \mathbb{D}(\mathcal{L}^+(A_i)) = \sum_{i=1}^n \sum_{t=1}^k \otimes_{j=1}^k (1_{j=t} \log(\mathbb{D}(A_{i_t}^{(j)})) + 1_{j \neq t} I_j) \quad (19)$$

$$= \sum_{t=1}^k \otimes_{j=1}^k (1_{j=t} \sum_{i=1}^n \log(\mathbb{D}(A_{i_t}^{(j)})) + 1_{j \neq t} I_j). \quad (20)$$

The summands are multiplicatively commutative, and so by proposition 2.3 of ([12]) and using the fact that for a continuous matrix valued function, $f(A \otimes I) = f(A) \otimes I$:

$$\exp\left(\sum_{t=1}^k \otimes_{j=1}^k (1_{j=t} \sum_{i=1}^n \log(\mathbb{D}(A_{it}^{(j)})) + 1_{j \neq t} I_j)\right) = \otimes_{j=1}^k \left(\exp[1_{j=t} \sum_{i=1}^n \log(\mathbb{D}(A_{it}^{(j)}))] + 1_{j \neq t} I_j\right),$$

hence, $\exp\{\sum_{i=1}^n \log \mathbb{D}(\mathcal{L}^+(A_i))\} \in \mathbb{D}^+(\mathbf{I}) = \mathbb{D}(\mathcal{L}^+(\mathbf{I}))$.

To show $\frac{1}{n} \sum_{i=1}^n \lfloor \mathcal{L}^+(A_i) \rfloor \notin \lfloor \mathcal{L}^+ \rfloor(\mathbf{I})$, without loss of generality suppose $\#(\mathbf{I}) = 2$. Further suppose that $\mathcal{L}^+(A_i) = \mathcal{L}^+(A_i^{(1)}) \otimes \mathcal{L}^+(A_i^{(2)})$. Then observe

$$\mathcal{L}^+(A_i) = (\lfloor \mathcal{L}^+(A_i^{(1)}) \rfloor + \mathbb{D}(\mathcal{L}^+(A_i^{(1)}))) \otimes (\lfloor \mathcal{L}^+(A_i^{(2)}) \rfloor + \mathbb{D}(\mathcal{L}^+(A_i^{(2)}))). \quad (21)$$

It must then be necessarily true if $B \in \lfloor \mathcal{L}^+ \rfloor(\mathbf{I})$ that $\exists C \in \mathcal{L}^+(d_1), D \in \mathcal{L}^+(d_2)$ such that:

$$B = \lfloor C \rfloor \otimes \lfloor D \rfloor + \lfloor C \rfloor \otimes \mathbb{D}(D) + \mathbb{D}(C) \otimes \lfloor D \rfloor. \quad (22)$$

Note that each of these components contribute independently to the strictly lower triangular elements of the lower triangular blocks, the strictly lower triangular elements of the lower triangular blocks, and the diagonal elements of the strictly lower triangular blocks, respectively.

Let Ψ denote any of these corresponding blocks of $P + Q$ for $P, Q \in \mathcal{L}^+(\mathbf{I})$ such that $P \neq Q$. Letting I denote the non-zero elements of P and Q , if $A + B$ were Kronecker structured, it must necessarily follow that for $\{i_1, j_1\}, \{s_1, t_1\} \in I$ such that

$$i_1, s_1, j_1, t_1 \in \{md_2 + 1, \dots, d_2(m+1)\}$$

where $m \in \{0, \dots, d_1 - 1\}$:

$$\frac{\Psi_{i_1, j_1}}{\Psi_{s_1, t_1}} = \gamma = \frac{P_{i_1, j_1} + Q_{i_1, j_1}}{P_{s_1, t_1} + Q_{s_1, t_1}}$$

letting $i_2, j_2, s_2, t_2 = i_1, j_1, s_1, t_1 + d_2$, assuming the corresponding element exists and is non-zero, it necessarily leads to

$$\frac{\Psi_{i_2, j_2}}{\Psi_{s_2, t_2}} = \gamma = \frac{P_{i_2, j_2} + Q_{i_2, j_2}}{P_{s_2, t_2} + Q_{s_2, t_2}}.$$

Assuming P, Q are the corresponding blocks of the matrices $A \otimes B, C \otimes D$, respectively,

$$\begin{aligned} P_{i_1, j_1} &= a_1 b_{i,j}, & P_{i_2, j_2} &= a_2 b_{i,j}, & Q_{i_1, j_1} &= c_1 d_{i,j}, & Q_{i_2, j_2} &= c_2 d_{i,j} \\ P_{s_1, t_1} &= a_1 b_{s,t}, & P_{s_2, t_2} &= a_2 b_{s,t}, & Q_{s_1, t_1} &= c_1 d_{s,t}, & Q_{s_2, t_2} &= c_2 d_{s,t} \end{aligned}$$

it would then follow:

$$\frac{a_1 b_{i,j} + c_1 d_{i,j}}{a_1 b_{s,t} + c_1 d_{s,t}} = \frac{a_2 b_{i,j} + c_2 d_{i,j}}{a_2 b_{s,t} + c_2 d_{s,t}}.$$

However, this does not in general hold for arbitrary SPD matrices A, B, C, D . The general multiway case holds analogously. \square

Of importance is to note that it does not generally hold that Fréchet means on separable manifolds are always non-separable. For example, if $T_i \in \mathcal{P}^+(\mathbf{I})$, $\log(T_i) = \sum_{j=1}^k \otimes_{t=1}^k (1_{t=j} \log(A_t) + 1_{t \neq j} I_t)$. Given a finite sample $T_1, \dots, T_n \in \mathcal{P}^+(d)$, the log-Euclidean Fréchet mean is given by [32] as the following expression

$$\mu_{LE}(\{T_i\}_{i=1}^n) = \exp\left(\frac{1}{n} \sum_{i=1}^n \log(T_i)\right)$$

and as the summands of the exponent are multiplicatively commutative, it immediately holds $\mu_{LE}(\{T_i\}_{i=1}^n) \in \mathcal{P}^+(\mathbf{I})$. Moreover, while the Affine-Invariant metric has no closed-form Fréchet mean, we found a similar result numerically for it.

As an analog to Corollary 12 of [23], even though the result of Theorem 2.1 states that the Fréchet mean in multiway Cholesky space does not yield something which is Kronecker structured, the log determinant is still the geometric mean of the determinants,

Proposition 2.1. *Let L^\dagger be defined as in Theorem 2.1, then*

$$\det L^\dagger = \exp\left(\sum_{i=1}^n \sum_{j=1}^k d_{-j} \log \det L_i^{(j)}\right).$$

Proof. The result is a direct extension of Corollary 13 in [23], where we additionally recognize $\log |L_i| = \sum_{j=1}^k d_{-j} \log |L_i^{(j)}|$. \square

Here, in particular, the emphasis is that $\mathbb{E}_n(L_1, \dots, L_n) \notin \mathcal{L}^+(\mathbf{I})$. The key point is that the diagonal still exists in Kronecker space; hence the determinant of the Fréchet mean is expressible as

a decomposition in terms of determinants of the components. However, because the strictly lower triangular part cannot be appropriately expressed in Kronecker product form, it cannot exist as a single Kronecker product.

2.2 Enhancing The Tensor Normal

The classical covariance parametrization of the d dimensional multivariate normal density is given by:

$$f(x|\Sigma, \mu) = \frac{1}{(2\pi)^{d/2} |\Sigma|^{\frac{1}{2}}} \exp\left(-\frac{1}{2}(x - \mu)\Sigma^{-1}(x - \mu)\right). \quad (23)$$

Equivalently, representing this density with the precision matrix, $\Theta = \Sigma^{-1}$, yields

$$f(x|\Sigma, \mu) = \frac{|\Theta|^{\frac{1}{2}}}{(2\pi)^{d/2}} \exp\left(-\frac{1}{2}(x - \mu)\Theta(x - \mu)\right). \quad (24)$$

Alternatively applying the Cholesky decomposition of the precision matrix, $\Theta = L_\theta L_\theta^T$, the density becomes

$$f(x|L_\theta, \mu) = \frac{|L_\theta|}{(2\pi)^{d/2}} \exp\left(-\frac{1}{2}(x - \mu)L_\theta L_\theta^T(x - \mu)\right). \quad (25)$$

Now let $T = \{L_1, \dots, L_n\}$ such that each $L_i \in \mathcal{L}^+(\mathbf{I})$ such that $\#(\mathbf{I}) = 2$. Using the results of the previous section, let L^\dagger have the same meaning as in (17):

$$f(x|T, \mu) = \frac{|L^\dagger|}{(2\pi)^{d/2}} \exp\left(-\frac{1}{2}(x - \mu)L^\dagger(L^\dagger)^T(x - \mu)\right). \quad (26)$$

Which by Proposition 2.1 yields:

$$f(x|T, \mu) = \frac{\exp(\sum_{i=1}^n \sum_{j=1}^k d_{-j} \log \det L_i^{(j)})}{(2\pi)^{d/2}} \exp\left(-\frac{1}{2}(x - \mu)(x - \mu)^T\right) \quad (27)$$

$$\left[\sum_{i=1}^n [\mathcal{L}(A_i)] + \exp\left\{ \sum_{i=1}^n \log \mathbb{D}(\mathcal{L}(A_i)) \right\} \right] \left[\sum_{i=1}^n [\mathcal{L}(A_i)] + \exp\left\{ \sum_{i=1}^n \log \mathbb{D}(\mathcal{L}(A_i)) \right\} \right]^T. \quad (28)$$

Note that we can further simplify this likelihood to involve only the constituent components of the Kronecker product. Specifically, in the case $\#(\mathbf{I}) = 2$, we can say $A_i = A_1^{(i)} \otimes A_2^{(i)}$, in which

case $\mathcal{L}(A_i) = \mathcal{L}(A_1^{(i)} \otimes A_2^{(i)}) = \mathcal{L}(A_1^{(1)}) \otimes \mathcal{L}(A_1^{(2)})$. By the same reasoning as (21) - (22):

$$\begin{aligned}\mathcal{L}(A_1^{(i)}) \otimes \mathcal{L}(A_2^{(i)}) &= [\lfloor \mathcal{L}(A_1^{(i)}) \rfloor + \mathbb{D}(\mathcal{L}(A_1^{(i)}))] \otimes [\lfloor \mathcal{L}(A_2^{(i)}) \rfloor + \mathbb{D}(\mathcal{L}(A_2^{(i)}))] \\ \implies \lfloor \mathcal{L}(A_i) \rfloor &= \lfloor \mathcal{L}(A_1^{(i)}) \rfloor \otimes \lfloor \mathcal{L}(A_2^{(i)}) \rfloor + \mathbb{D}(\mathcal{L}(A_1^{(i)})) \otimes \lfloor \mathcal{L}(A_2^{(i)}) \rfloor + \lfloor \mathcal{L}(A_1^{(i)}) \rfloor \otimes \mathbb{D}(\mathcal{L}(A_2^{(i)})) \\ \mathbb{D}(\mathcal{L}(A_i)) &= \mathbb{D}(\mathcal{L}(A_1^{(i)})) \otimes \mathbb{D}(\mathcal{L}(A_2^{(i)})).\end{aligned}$$

Moreover, it's straightforward to see that

$$\left[\sum_{i=1}^n \lfloor \mathcal{L}(A_i) \rfloor + \exp \left\{ \sum_{i=1}^n \log \mathbb{D}(\mathcal{L}(A_i)) \right\} \right]^T = \sum_{i=1}^n \lfloor \mathcal{L}(A_i) \rfloor^T + \exp \left\{ \sum_{i=1}^n \log \mathbb{D}(\mathcal{L}(A_i)) \right\}.$$

For brevity of this section, we will refrain from the full computation of the likelihood until the supplemental computational details are provided in Section 8.

This parameterization allows for a more general representation of Cholesky factors than the more straightforward argument of separability. In particular, as stated in Theorem 2.1, a general Cholesky factor, L , can only be adequately represented with a multiway Cholesky factorization when it is strictly lower triangular elements then

$$\frac{L_{i_1, j_1}}{L_{s_1, t_1}} = \frac{L_{i_2, j_2}}{L_{s_2, t_2}}.$$

However, under our parameterization, we are able to circumvent this structural assumption, as observed in the following Lemma for the matrix normal case.

Lemma 2.2. *Let $\Psi \in \mathbb{R}^{d_1 d_2 \times d_1 d_2}$ be an arbitrary strictly lower triangular matrix such that*

$$\Psi_{d_2 r + v, d_2 s + w} = 0$$

if $r > s$ or $w > v$. Then

$$\arg \min_{A, B} \|\Psi - A \otimes B\|_F \in \lfloor \mathcal{L}^+ \rfloor(d_1) \times \lfloor \mathcal{L}^+ \rfloor(d_2).$$

Proof. Assuming $A, B \in \mathbb{R}^{d_1 \times d_1} \times \mathbb{R}^{d_2 \times d_2}$ are unconstrained, this is a direct result of the following

calculations:

$$\begin{aligned}
\|\Psi - A \otimes B\|_F^2 &= \sum_{i=1}^{d_1 d_2} \sum_{j=1}^{d_1 d_2} |\Psi_{i,j} - [A \otimes B]_{i,j}|^2 \\
&= \sum_{r=1}^{d_1-1} \sum_{s=1}^{d_1-1} \sum_{v=1}^{d_2} \sum_{w=1}^{d_2} |\Psi[d_2 r + v, d_2 s + w] - [A \otimes B][d_2 r + v, d_2 s + w]|^2 \\
&= \sum_{r \geq s} \sum_{v \geq w} |\Psi[d_2 r + v, d_2 s + w] - [A \otimes B][d_2 r + v, d_2 s + w]|^2 \\
&\quad + \sum_{r \geq s} \sum_{w < v} |A_{r,s} B_{v,w}|^2 + \sum_{r < s} \sum_{w \geq v} |A_{r,s} B_{v,w}|^2 + \sum_{r \leq s} \sum_{w \leq v} |A_{r,s} B_{v,w}|^2.
\end{aligned}$$

The last line follows from $(A \otimes B)_{d_2 r + v, d_2 s + w} = A_{r,s} B_{v,w}$ and merely penalizes non-strictly lower triangular elements of A and B . Hence, $\|\Psi - A \otimes B\|_F^2$ is minimized when A and B are lower triangular. \square

By the works of [26] and [33], it is analogous that then by iterating this process on the residuals of $\Psi - A \otimes B$ for strictly lower triangular Ψ , there exists a collection of matrices $\{A_i, B_i\}_{i=1}^{r^2}$ where $r = \min\{d_1, d_2\}$ such that

$$\|\Psi - \sum_{i=1}^{r^2} A_i \otimes B_i\|_F = 0. \quad (29)$$

We refer to this representation as a sum of Kronecker products as the Pitsianis-Van Loan (P-VL) decomposition.

Then analogously with respect to the general capability of representing an arbitrary Cholesky factorization of a precision matrix through a Fréchet mean of separable Cholesky factors, we observe the following lemma:

Lemma 2.3. *Let $L^\dagger = \mu_{LC}(\{\otimes_{i=1}^2 L_i^{(j)}\}_{j=1}^K)$ be the Cholesky Fréchet mean of a K -collection of multiway Cholesky factors where $K = \min\{d_1^2, d_2^2\}$ such that $\mathbb{D}(\otimes_{i=1}^2 L_i^{(p)}) = \mathbb{D}(\otimes_{i=1}^2 L_i^{(q)})$ for $p \neq q$, then for arbitrary $L \in \mathcal{L}^+(d_1 d_2)$:*

$$\min_{L^\dagger} \|L^\dagger - L\|_F \leq \sqrt{\sum_{r > s} \sum_{v > w} L_{d_2 r + v, d_2 s + w}^2} + D_2(L).$$

where $D_2(L)$ is the second largest diagonal of L .

Proof. By triangle inequality,

$$\|L^\dagger - L\|_F \leq \| \lfloor L^\dagger \rfloor - \lfloor L \rfloor \|_F + \|\mathbb{D}(L^\dagger) - \mathbb{D}(L)\|_F$$

First note that by iteratively minimizing the residuals of $\Psi - A \otimes B$ for Ψ has the sparsity structure of Lemma (2.2), through the argument of the P-VL decomposition, it immediately follows by a second application of triangle inequality:

$$\begin{aligned} \min_{L^\dagger} \|L^\dagger - L\|_F &\leq \sqrt{\sum_{r>s} \sum_{v>w} L_{d_2r+v, d_2s+w}^2} + \min_{L^\dagger} \sqrt{\sum_{r\leq s} \sum_{v\leq w} L_{d_2r+v, d_2s+w}^2 - L_{d_2r+v, d_2s+w}^\dagger} \\ &= \sqrt{\sum_{r>s} \sum_{v>w} L_{d_2r+v, d_2s+w}^2} \end{aligned}$$

where the second line follows for sufficiently large K by equation (29). By a secondary application of P-VL it also follows:

$$\min_{L^\dagger} \|\mathbb{D}(L^\dagger) - \mathbb{D}(L)\| = \min_{D_1, D_2} \|\otimes_{i=1}^d D_i - \mathbb{D}(L)\| \leq D_2(L).$$

□

Observe the implication of the above Lemma is that we can arbitrarily represent strictly lower triangular matrices through an analogue of the P-VL decomposition given the matrix has an appropriate sparsity structure (specifically, the lower triangular sparsity structure introduced from multiway Cholesky factors).

3 The Bayesian Model

The model of [18] provides an excellent starting point for adequately structuring an appropriate Bayesian model for multiway data. Assuming that

$$y_1, \dots, y_n \sim N(0, \otimes_{i=1}^D \Sigma_i).$$

Given a lack of scale identifiability in any of the components present in the data:

$$(cA) \otimes \left(\frac{1}{c}B\right) = A \otimes B$$

the authors propose to estimate the $\{\Sigma_i\}_{i=1}^D$ by means of centering the prior expectations of the covariance:

$$\Sigma_i \sim IW(d_i + 2, \frac{\gamma^{\frac{1}{D}}}{d_i} I_{d_i})$$

such that $\gamma = \text{tr}(\frac{1}{n-1} \sum_{i=1}^n y_i y_i^T)$. The central point of this argument being that the prior centering of the covariance allows one to argue:

$$\mathbb{E}[\text{tr}(\otimes_{i=1}^D \Sigma_i)] = \text{tr}(\mathbb{E}[\otimes_{i=1}^D \Sigma_i]) = \prod_{i=1}^D \frac{\gamma^{\frac{1}{D}}}{d_i} \text{tr}(I_{d_i}) = \gamma.$$

Consequently, there is little information in the structure of the individual $\{\Sigma_i\}$ present in the data itself, but we can use the linearity of the trace to provide a motivating relationship between our prior expectations and the trace of the sample covariance matrix. Directly extending such a summation directly to the Fréchet mean would necessarily then require finding a parameterization for centering:

$$\mathbb{E}[\text{tr}(\exp(D))] = \mathbb{E}[\exp(|D|)].$$

In the next section, we instead parameterize $\exp(D_1) \otimes \exp(D_2)$ directly with priors with only positive support.

3.1 Centering Matrix Priors

In this section we will introduce several auxiliary results used in the construction of Bayesian models in Sections 3.2 and 3.3.

Lemma 3.1. *Suppose $c > 1$ and let $\alpha(c)$ be the solution to $f(x) = c \exp(-\frac{2}{x}) - 1 - \frac{1}{x}$. If $\alpha(c)$ is large enough to satisfy $\alpha(c) + \alpha^2(c) < \frac{\epsilon}{\exp(\frac{1}{\alpha}) - 1}$, then $|\alpha^2 + \alpha - c \exp(2\psi_0(\alpha))| < \epsilon$.*

Proof. For $x > 0$, a known bound on the digamma function is given by:

$$\psi_0(x) \in (\log(x) - \frac{1}{x}, \log(x) - \frac{1}{2x}). \quad (30)$$

It follows:

$$-c \exp(2\psi_0(x)) \in \left(-cx^2 \exp(-\frac{1}{x}), -cx^2 \exp(-\frac{2}{x}) \right).$$

Then we can bound

$$x^2 + x - c \exp(2\psi_0(x)) \in \left(x^2(1 - c \exp(-\frac{1}{x})) + x, x^2(1 - c \exp(-\frac{2}{x})) + x \right) = (l(x), u(x))$$

For $x > 0$, $u(x) = 0$ occurs when

$$c \exp(-\frac{2}{x}) - 1 = \frac{1}{x}. \quad (31)$$

Note that the right-hand side is positive and strictly decreasing in x , while the left-hand side is continuous and strictly increasing with corresponding limits -1 and $c - 1$ as $x \rightarrow 0$ and $x \rightarrow \infty$, respectively, for any $c > 0$, so a solution must exist. Letting α be the solution to (31), it follows that

$$w(\alpha) = u(\alpha) - l(\alpha) = \alpha^2 c \left(\exp(-\frac{1}{\alpha}) - \exp(-\frac{2}{\alpha}) \right). \quad (32)$$

Note that from the solution to (31), it must follow $c \exp(-\frac{2}{\alpha}) = \frac{1+\alpha}{\alpha}$, and therefore

$$w(\alpha) = \alpha^2 \left(\frac{1+\alpha}{\alpha} \left(\exp(\frac{1}{\alpha}) - 1 \right) \right) = (\alpha + \alpha^2) \left(\exp(\frac{1}{\alpha}) - 1 \right).$$

From which if $\alpha(c)$ satisfies the conditions $w(\alpha) < \epsilon$ and $u(\alpha) = 0$, where we can deduce $|f(\alpha)| \leq u(\alpha) + w(\alpha) < \epsilon$. \square

Proposition 3.1. *Let $D_1 \in \mathbb{D}(d_1)$, $D_2 \in \mathbb{D}(d_2)$ be independently parameterized by:*

$$D_i[j_i, j_i] \sim \Gamma(a_i, \exp(\psi_0(a_i) - \frac{\gamma_D}{2d_1 d_2})), \quad j_i \in \{1, \dots, d_i\}$$

such that $a_i^2 + a_i - c_i \exp(2\psi_0(a_i)) = \epsilon$ for $c_i = \frac{\sqrt{F_D}}{d_i} \exp(-\gamma_D/(2d_1 d_2))$ for constant F_D, γ_D , then

$$\mathbb{E}[\log |D_1 \otimes D_2|] = \gamma_D \quad (33)$$

and

$$\mathbb{E}[\|D_1 \otimes D_2\|_F^2] = (\sqrt{F_D} + \frac{d_1 \epsilon}{\exp(-\frac{\gamma_D}{2}) \exp(2\psi_0(a_1))})(\sqrt{F_D} + \frac{d_2 \epsilon}{\exp(-\frac{\gamma_D}{2}) \exp(2\psi_0(a_2))}). \quad (34)$$

Proof. Note first that if $X \sim \Gamma(a, b)$, with rate b , it's known that

$$\mathbb{E}[\log(X)] = \psi(a) - \log(b) \quad (35)$$

and moreover

$$\mathbb{E}[X^2] = \frac{a + a^2}{b^2}. \quad (36)$$

Now note that

$$\log |D_1 \otimes D_2| = d_2 \log |D_1| + d_1 \log |D_2| \quad (37)$$

and observe by (35):

$$\log |D_i| = \sum_{j=1}^{d_i} \log D_i[j, j] \implies \mathbb{E}[\log |D_i|] = \sum_{j=1}^{d_i} [\psi_0(a_i) - \psi_0(a_i) + \frac{\gamma_D^{\frac{1}{2}}}{d_1 d_2}] = \frac{\gamma_D}{d_{-i}}.$$

By linearity, it follows from equation (37) that

$$\mathbb{E}[\log |D_1 \otimes D_2|] = \gamma_D.$$

To show that (34), note another convenient property of Kronecker products:

$$\|A \otimes B\|_F^2 = \|A\|_F^2 \|B\|_F^2 \quad (38)$$

for general matrices A, B . It follows that

$$\|D_1 \otimes D_2\|_F^2 = \|D_1\|_F^2 \|D_2\|_F^2.$$

Further observe that

$$\mathbb{E}[\|D_i\|_F^2] = \frac{1}{\exp(-\frac{\gamma_D}{d_1 d_2})} \sum_{j=1}^{d_i} \frac{a_i^2 + a_i}{\exp(2\psi_0(a_i))}$$

given $a_i^2 + a_i - c_i \exp(2\psi_0(a_i)) < \epsilon$. It then follows that

$$\frac{1}{\exp(-\frac{\gamma_D}{d_1 d_2})} \sum_{j=1}^{d_i} \frac{a_i^2 + a_i}{\exp(2\psi_0(a_i))} = \frac{1}{\exp(-\frac{\gamma_D}{d_1 d_2})} d_i (c_i + \frac{\epsilon}{\exp(2\psi_0(a_i))}).$$

Given that

$$\frac{1}{\exp(-\frac{\gamma_D}{d_1 d_2})} d_i c_i = \sqrt{F_D}$$

the result immediately follows by independence of D_1, D_2 . \square

Given that ϵ is arbitrary, we will resort to the notation of \approx to signify a precision up to ϵ . With this notation and Proposition 3.1, we can parameterize the strictly lower triangular entries as follows:

Theorem 3.2. *Let L_1, L_2 be positive definite Cholesky factors. Suppose $\mathcal{D}(L_1) \in \mathbb{D}(d_1)$, $\mathcal{D}(L_2) \in \mathbb{D}(d_2)$ be parameterized according to Proposition 3.1, further suppose the lower triangular entries are independently distributed according to*

$$\lfloor L_1 \rfloor[i, j] \sim N(0, \sigma^2 = \beta) \tag{39}$$

$$\lfloor L_2 \rfloor[p, q] \sim N(0, \sigma^2 = \beta) \tag{40}$$

with

$$\beta = \frac{-M_1 \sqrt{F_D}(1 + 1/c) + \sqrt{F_D(1 + 1/c)^2 + 4((M_1)^2/c) * F_L})}{(2 * M_1^2/c)} \tag{41}$$

$c = \frac{d_1(d_1-1)}{d_2(d_2-1)}$ and $M_1 = \frac{d_1(d_1-1)}{2}$, then

$$\mathbb{E}[\|\lfloor L_1 \otimes L_2 \rfloor\|_F^2] \approx F_L.$$

Proof. First observe that for $L_1 \in \mathcal{L}^+(d_1)$, $L_2 \in \mathcal{L}^+(d_2)$,

$$\lfloor L_1 \otimes L_2 \rfloor = \lfloor L_1 \rfloor \otimes \mathcal{D}(L_2) + \mathcal{D}(L_1) \otimes \lfloor L_2 \rfloor + \lfloor L_1 \rfloor \otimes \lfloor L_2 \rfloor = M_1 + M_2 + M_3.$$

Observe M_1, M_2, M_3 respectively contribute structurally to the strictly lower triangular entries of the diagonal blocks, the diagonals of the strictly lower triangular blocks, and the strictly lower tri-

angular components of the strictly lower triangular blocks. As such, letting \odot denote the Hadamard product, then $M_i \odot M_j = 0$ for $i \neq j$ and note that in general, if $A \odot B = 0$ for arbitrary matrices A, B compatible for such a multiplication, then $\|A + B\|_F^2 = \|A\|_F^2 + \|B\|_F^2$. It then follows that

$$\|\lfloor L_1 \otimes L_2 \rfloor\|_F^2 = \|\lfloor L_1 \rfloor \otimes \mathcal{D}(L_2)\|_F^2 + \|\mathcal{D}(L_1) \otimes \lfloor L_2 \rfloor\|_F^2 + \|\lfloor L_1 \rfloor \otimes \lfloor L_2 \rfloor\|_F^2$$

and by (38),

$$\|\lfloor L_1 \otimes L_2 \rfloor\|_F^2 = \|\lfloor L_1 \rfloor\|_F^2 \|\mathcal{D}(L_2)\|_F^2 + \|\mathcal{D}(L_1)\|_F^2 \|\lfloor L_2 \rfloor\|_F^2 + \|\lfloor L_1 \rfloor\|_F^2 \|\lfloor L_2 \rfloor\|_F^2.$$

Further suppose that we have element-wise independent priors on $\lfloor L_1 \rfloor$ as

$$\lfloor L_1 \rfloor[i, j] \sim N(0, \sigma^2 = \xi^2)$$

then it follows that

$$\mathbb{E}[\|\lfloor L_1 \rfloor\|_F^2] = \frac{d_1(d_1 - 1)}{2} \xi^2.$$

Further assuming

$$\mathbb{E}[\|L_1\|_F^2] = c \mathbb{E}[\|L_2\|_F^2]$$

then it is natural to assume

$$\lfloor L_2 \rfloor[p, q] \sim N(0, \sigma^2 = \frac{\xi^2}{c}),$$

then it follows that

$$\mathbb{E}[\|\lfloor L_2 \rfloor\|_F^2] = c \frac{d_1(d_1 - 1)}{2} \xi^2 = \frac{d_2(d_2 - 1)}{2} \xi^2.$$

Then by assuming $\lfloor L_1 \rfloor \lfloor L_2 \rfloor$ have priors independent of $\mathcal{D}(L_1)$, $\mathcal{D}(L_2)$, and letting

$$M_1 = \frac{d_1(d_1 - 1)}{2}$$

it then follows that

$$\begin{aligned}\mathbb{E}[\|\lfloor L_1 \otimes L_2 \rfloor\|_F^2] &= \mathbb{E}[\|\lfloor L_1 \rfloor\|_F^2]\mathbb{E}[\|\mathcal{D}(L_1)\|_F^2] + \mathbb{E}[\|\mathcal{D}(L_1)\|_F^2]\mathbb{E}[\|\lfloor L_2 \rfloor\|_F^2] + \mathbb{E}[\|\lfloor L_1 \rfloor\|_F^2]\mathbb{E}[\|\lfloor L_2 \rfloor\|_F^2] \\ &\approx F_D^{\frac{1}{2}}(\mathbb{E}[\|\lfloor L_1 \rfloor\|_F^2] + \mathbb{E}[\|\lfloor L_2 \rfloor\|_F^2]) + \mathbb{E}[\|\lfloor L_1 \rfloor\|_F^2]\mathbb{E}[\|\lfloor L_2 \rfloor\|_F^2]\end{aligned}\quad (42)$$

$$= F_D^{\frac{1}{2}}M_1(1 + \frac{1}{c})\xi + \frac{M_1^2}{c}\xi^2 \quad (43)$$

where (42) follows from Proposition 3.1. Further by assuming $\mathbb{E}[\|\lfloor L_1 \otimes L_2 \rfloor\|_F^2] = F_L$, it then follows from (43) that

$$F_D^{\frac{1}{2}}M_1(1 + \frac{1}{c})\xi + \frac{M_1^2}{c}\xi^2 = F_L$$

and solving the quadratic equation in ξ yields (41). \square

Corollary 3.1. *Suppose $\{L_1^{(i)}, L_2^{(i)}\}_{i=1}^K$ be positive definite Cholesky factors such that $\{\mathbb{D}(L_1^{(i)}), \mathbb{D}(L_2^{(i)})\} = \{D_1, D_2\}$ for all i , and let L be the Cholesky factor defined by*

$$L = \sum_{i=1}^K \lfloor L_1^{(i)} \otimes L_2^{(i)} \rfloor + D_1 \otimes D_2$$

with D_1, D_2 parameterized according to Proposition 3.1, and

$$\lfloor L_1^{(i)} \rfloor[i, j] \sim N(0, \sigma^2 = \omega_i \beta) \quad (44)$$

$$\lfloor L_2^{(i)} \rfloor[p, q] \sim N(0, \sigma^2 = \omega_i \beta) \quad (45)$$

such that $\Omega = (\omega_1, \dots, \omega_K) \in \Delta^K$ is distributed on the unit simplex and β is from Theorem 3.2, then

$$\mathbb{E}[\|\lfloor L \rfloor\|_F^2] = F_L. \quad (46)$$

Proof. First note that

$$\begin{aligned}\mathbb{E}[\|\lfloor L_1 \otimes L_2 \rfloor\|_F^2] &= \mathbb{E}[\|\sum_i \lfloor L_1^{(i)} \rfloor\|_F^2 \|D_2\|_F^2 + \|D_1\|_F^2 \|\sum_i \lfloor L_2^{(i)} \rfloor\|_F^2] \\ &\quad + \mathbb{E}[\|\sum_i \lfloor L_1^{(i)} \rfloor\|_F^2 \|\sum_i \lfloor L_2^{(i)} \rfloor\|_F^2].\end{aligned}$$

Note also that if $\{A_i\}_{i=1}^K$ are random matrices such that $A_i \stackrel{d}{=} \alpha_i A$ for independent random variables $\{\alpha_i\}_{i=1}^K, A$:

$$\sum_{i=1}^K A_i \stackrel{d}{=} \sum_{i=1}^K \alpha_i A$$

and therefore it follows that

$$\left\| \sum_{i=1}^K A_i \right\|_F^2 \stackrel{d}{=} \left\| \sum_{i=1}^K \alpha_i A \right\|_F^2 = \left(\sum_{i=1}^K \alpha_i \right)^2 \|A\|_F^2.$$

Let $\lfloor S_j \rfloor$ denote a $d_j \times d_j$ strictly lower triangular matrix with standard normal entries. Note $\|S_j\|_F^2 \sim \chi_{d_j(d_j-1)/2}^2$ and $\|L_1^{(j)}\|_F^2 \|L_2^{(j)}\|_F^2 \stackrel{d}{=} (\omega_i \beta)^2 Q$, where $Q \sim \|\lfloor S_1 \rfloor\|_F^2 \|\lfloor S_2 \rfloor\|_F^2$ for independent S_1, S_2 . From this, it is clear that

$$\mathbb{E}[\|\lfloor \sum_i L_j^{(i)} \rfloor\|_F^2] = \mathbb{E}[\mathbb{E}[\|\lfloor \sum_i L_j^{(i)} \rfloor\|_F^2 | \Omega]] = \mathbb{E}[\mathbb{E}[(\sum_i \omega_i \sqrt{\beta})^2 \|\lfloor S_j \rfloor\|_F^2 | \Omega]] = \beta \mathbb{E}[\|\lfloor S_j \rfloor\|_F^2].$$

From Theorem 3.2, it follows $\mathbb{E}[\|\lfloor L \rfloor\|_F^2] = \beta$. □

3.2 Non-Dynamic Bayesian Model Selection

Expressing the model formulation above more compactly, the full Sum of Cholesky factor Kronecker Product Decomposition (SCKPD) Bayesian model is specified as

$$\begin{aligned} y_1, \dots, y_N &\sim N(0, L^\dagger (L^\dagger)^T) \\ L^\dagger [\{L_1^{(i)}, L_2^{(i)}\}_{i=1}^K, D_1, D_2] &= \sum_{i=1}^K \lfloor L_1^{(i)} \otimes L_2^{(i)} \rfloor + D_1 \otimes D_2 \\ D_i | a_i, \gamma_D &\sim \Gamma\left(a_i, \exp(\psi_0(a_i) - \frac{\gamma_D}{2d_1 d_2})\right) \\ a_i &= \arg \min_{\xi} |\xi^2 + \xi - c_i \exp(2\psi_0(\xi))|, \quad c_i = \frac{\sqrt{F_D}}{d_i} \exp(-\frac{\gamma_D}{2d_1 d_2}) \\ \lfloor L_1^{(i)} \rfloor &\stackrel{D}{=} \lfloor L_2^{(i)} \rfloor | \Omega, \beta, F_D, F_L \sim N(0, \sigma^2 = \omega_i \beta), \\ \text{where } \beta &= \frac{-M_1 \sqrt{F_D} (1 + \frac{1}{c}) + \sqrt{F_D (1 + \frac{1}{c})^2 + 4(M_1^2/c) F_L}}{2M_1^2/c} \\ \Omega | \theta &\sim \mathcal{D}(\theta) \\ \theta &\sim U(0, 1) \end{aligned} \tag{47}$$

where $\Omega = (\omega_1, \dots, \omega_k)$, $\gamma_D = \log |\mathcal{L}(S)|$, $F_D = \|\mathbb{D}(\mathcal{L}(S))\|_F^2$, $F_L = \|\mathcal{L}(S)\|_F^2$ such that S is the sample covariance matrix, $c = \frac{d_1(d_1-1)}{d_2(d_2-1)}$, $M = \frac{d_1(d_1-1)}{2}$, and $\mathcal{D}(\theta)$ denotes the Dirichlet distribution with concentration parameter θ .

3.3 Seasonally Dynamic Covariance

In this section, we will provide a simple extension of the SCKPD Bayesian model (47) in the case where we have collections of observations with seasonal matrix values that have fixed observations within the season, but the correlation structure shifts between seasons. More specifically, we consider the case where we have observations that are generated from a finite collection of Cholesky factors $C = \{L_1^{(i)}, L_2^{(i)}\}_{i=1}^K$, where in season s in cycle c , the relative contributions of the elements in C to the precision matrix are constant for all $y_1^{(s,c)}, \dots, y_n^{(s,c)}$, and change as we move to $y_1^{(s+1,c)}, \dots, y_n^{(s+1,c)}$ or $y_1^{(s-S+1,c+1)}, \dots, y_n^{(s-S+1,c+1)}$. As we are considering the regime where the relative contributions shift but not the underlying covariances themselves, we provide a particularly simplistic form for the data generating process, which we term the Seasonally Dynamic sum of Cholesky factor Kronecker Product Decomposition (SD-SCKPD) Bayesian model:

$$\begin{aligned}
y_1^t, \dots, y_N^t &\sim N(0, L_t^\dagger (L_t^\dagger)^T) \\
L_t^\dagger | \{L_{1,t}^{(i)}, L_{2,t}^{(i)}\}_{i=1}^K, D_1, D_2 &= \sum_{i=1}^K [L_{1,t}^{(i)} \otimes L_{2,t}^{(i)}] + D_1 \otimes D_2 \\
D_i | a_i, \gamma_D &\sim \Gamma(a_i, \exp(\psi_0(a_i) - \frac{\gamma_D}{2d_1d_2})) \\
a_i &= \arg \min_{\xi} |\xi^2 + \xi - c_i \exp(2\psi_0(\xi))|, \quad c_i = \frac{\sqrt{F_D}}{d_i} \exp(-\frac{\gamma_D}{2d_1d_2}) \\
[L_{1,t}^{(i)}] &\stackrel{D}{=} [L_{2,t}^{(i)}] | \Omega_t, \beta, F_D, F_L \sim N(0, \sigma^2 = \omega_{i,t}\beta), \\
\text{where } \beta &= \frac{-M_1\sqrt{F_D}(1 + \frac{1}{c}) + \sqrt{F_D(1 + \frac{1}{c})^2 + 4(M_1^2/c)F_L}}{2M_1^2/c} \\
\Omega_1 | \theta &\sim \mathcal{D}(\theta) \\
\Omega_{t+1} &= A\Omega_t, \quad A \in \mathbb{R}_+^{K \times K}, \quad \sum_{j=1}^K A_{i,j} = 1 \\
\theta &\sim U(0, 1).
\end{aligned} \tag{48}$$

In this case, M_1, F_D, F_L, γ_D , and c maintain the same interpretation of the SCKPD model, but

restricted to the first season of observations y_1^1, \dots, y_N^1 . This extension introduces the stochastic matrix of nonnegative columns A to allow perturbations between Ω_t and Ω_{t+1} while maintaining the simplex constraint:

$$\sum_{k=1}^K (A\Omega_{t+1})_k = \sum_{i=1}^K \sum_{j=1}^K A_{i,j} \Omega_i = \sum_{i=1}^K \Omega_i = 1.$$

Such a model can be useful for cases where data may exhibit varying degrees of deeply correlated residual structure to varying degrees during different seasons. As we emphasize the use of this model in modeling seasonality effects, we can equivalently state that for $\Omega(0) = \Omega$, it follows that at season s in cycle c :

$$\Omega(s, c) = A^{c+s-1} \Omega$$

Note that such a prior assumes that the covariance exhibits a temporal relationship in $\Sigma_t = L_t^\dagger [L_t^\dagger]^T$ such that

$$\begin{aligned} \mathbb{E}[tr(\Theta_t)] &= \mathbb{E}\left[\sum_i (L_{ii}^\dagger)^2 + \sum_i \sum_{j>i} (L_{i,j}^\dagger)^2\right] = \mathbb{E}[\|\mathbb{D}(L^\dagger)\|_F^2] + \mathbb{E}[\|L^\dagger\|_F^2] = F_D + F_L \\ \mathbb{E}[\log |\Theta_t|] &= \gamma_D \end{aligned}$$

Implicates a temporal evolution where the total variance and eigenvalues' geometric mean is fixed across time states. This however is only a restriction on the magnitudes of variation, rather than the directions, allowing for flexibility in modeling directions of regime shifts in cases where a time series may effectively exhibit patterns where variability of a vector time series is "passed" between it's elements through a temporal evolution.

4 Implementation Details

We sample the SCKPD model using Hamiltonian Monte Carlo. However, this poses two options: to convert to an unconstrained parameterization for sampling, as is done with `stan`, or to use a geometrically informed implementation such as geodesic Monte Carlo ([19, 28, 4]). Under the

log-Cholesky metric, the geodesic connecting $L_0 = \mathcal{L}(P_0)$ to $L_1 = \mathcal{L}(P_1)$ is given by [23]:

$$\begin{aligned} & \lfloor L_0 \rfloor + t(\lfloor L_1 \rfloor - \lfloor L_0 \rfloor) + \mathbb{D}(L_0) \exp(t\mathbb{D}(L_0) \log(\mathbb{D}(L_0)^{-1}\mathbb{D}(L_1)))\mathbb{D}(L_0)^{-1} \\ &= \lfloor L_0 \rfloor + t(\lfloor L_1 \rfloor - \lfloor L_0 \rfloor) + \mathbb{D}(L_1)^t \mathbb{D}(L_0)^{1-t}. \end{aligned}$$

A consideration in using a geodesic implementation is the potential efficiency gained by the Riemannian analogue of Euclidean convexity, as was discovered for multiway covariances of Gaussian arrays in [34].

Definition 4.1. Let (\mathcal{M}, g) be a Riemannian manifold. A function f defined on \mathcal{M} is geodesically convex if for all $p, q \in \mathcal{M}$:

$$f(\gamma(t)) \leq tf(\gamma(0)) + (1-t)f(\gamma(1))$$

where $\gamma(t)$ is the geodesic such that $\gamma(0) = p$, $\gamma(1) = q$.

However, as an extension of Lemma 3 of ([34]), we show that the inner product for vectorized tensor normal observations is not jointly geodesically convex under a product manifold geometry for the log-Cholesky metric.

Lemma 4.2. Let $\mathbb{C}_n = \mathcal{C}_1 \times \mathcal{C}_2 \times \cdots \times \mathcal{C}_n$ denote the product manifold of $\{\mathcal{C}_i\}_{i=1}^n$, independently endowed with the Cholesky metric. That is, each element is the n -tuple pair, $\mathcal{M} = (\times_{i=1}^n \mathcal{C}_i, \oplus G(\mathcal{C}_i))$. Suppose $h \in \mathbb{R}^n$, then $h^T L L^T h$ is not geodesically convex in $\times_{i=1}^D L_i \in \mathcal{M}$.

Proof. Suppose $L_1 \in \mathcal{C}^n, L_2 \in \mathcal{C}^m$. For the Kronecker product of Cholesky factors,

$$h^T (L_1(t) \otimes L_2(t)) (L_1(t) \otimes L_2(t))^T h = \sum_i y_i(t) \quad (49)$$

$$y_i(t) = \sum_{j=1}^i [(L_1(t) \otimes L_2(t))_{i,j} h_j]^2. \quad (50)$$

Noting that

$$(L_1(t) \otimes L_2(t))_{mj+s, mq+t} = (L_1(t))_{j,q} (L_2(t))_{s,t}, \quad 1 \leq j, q \leq n-1, \quad 1 \leq s, t \leq m.$$

Results in:

$$y_{mj+s}(t) = \sum_{0 \leq (a,b) \leq (j,s)} ([L_1(t)]_{j,a}^2 [L_2(t)]_{s,b}^2 h_{ma+b}^2) \quad (51)$$

where

$$[L_i(t)]_{x,y} = \begin{cases} (1-t)[L_i(0)]_{x,y} + t[L_i(1)]_{x,y} & \text{if } x \neq y \\ \mathbb{D}_x(L_i(0))^{1-t} \mathbb{D}_x(L_i(1))^t & \text{if } x = y \end{cases}$$

$$\implies [L_i(t)]_{x,y}^2 = \begin{cases} (1-t)^2 [L_i(0)]_{x,y}^2 + t^2 [L_i(1)]_{x,y}^2 + 2(1-t)t [L_i(0)]_{x,y} [L_i(1)]_{x,y} & \text{if } x \neq y \\ \mathbb{D}_x(L_i(0))^{2(1-t)} \mathbb{D}_x(L_i(1))^{2t} & \text{if } x = y. \end{cases}$$

Then any element of y gives no guarantee of convexity, as we cannot guarantee positivity, nor strictly increasing/decreasing in any of the entries due to any second-order or higher terms containing products of unconstrained lower triangular elements. Hence, the function is certainly not jointly geodesically convex in this space. \square

Practically, Lemma 4.2 states that if we follow Riemannian gradients under the product manifold geometry of Cholesky factors for just a single Kronecker product alone, it is not a geodesically convex path. One could potentially use parallel tempering as an attempt to alleviate the non-convexity. However, this would not be of great benefit when off the shelf Hamiltonian Monte Carlo samplers such as **stan** exist with built-in tuning mechanisms for efficiency.

For implementation with **stan**, gradients are instead computed with respect to unconstrained parameterizations of $L_i^{(j)}$. We need not deal directly with the conversion of constrained lower triangular matrices to an unconstrained space, which is handled internally within **stan**. However, it would be important to consider alternative forms of the likelihood for efficiency. In Section 8, we cover implementation details for efficient computation and parallelization of **stan**'s computing environment for Bayesian SCKPD model.

However, one note is that the estimation of A for the dynamic covariance model of Section 3.3: **stan** does not allow directly placing priors on the columns of a matrix parameter. In each example considered within this paper, we assume that the columns are iid distributed according to

a $\mathcal{D}(\alpha \mathbf{1}_k)$. By [6], we can instead treat A as a transformed parameter:

$$A[i, j] | A^* = \frac{A^*[i, j]}{\sum_j A^*[i, j]}$$

$$A_{i,j} \stackrel{iid}{\sim} \Gamma(\alpha, 1)$$

5 Simulated Data Examples

In this section we will consider simulated data examples to assess our model's ability to recover the true data generating process.

5.1 Static Covariance

In our first simulation, we consider the fixed mean case where the true data generating process is simulated according to:

$$y \sim N(0, \Theta = L^\dagger [L^\dagger]^T)$$

$$L^\dagger = \sum_{j=1}^K [L_1^{(i)} \otimes L_2^{(i)}] + D_1 \otimes D_2$$

$$[L_1^{(i)}] \stackrel{d}{=} [L_2^{(i)}] \sim N(0, \omega_i \beta)$$

with $\beta = 2$, $\Omega = \frac{\Omega_u}{\sum_j \Omega_u[j]}$ where $\Omega_u = (1, 4, 6, 7, 9)$. In the first 3 simulation examples, we generate data and fit the SCKPD Bayesian model according to:

- $r = k = 5$ (perfect association of true separability rank and data generating separability rank)
- $r = 5, k = 8$ (overspecification of separability rank)
- $r = 1, k = 5$ (overspecification of separability rank under a truly separable data generating process)

In all three examples, $\dim(A) = 5$, $\dim(B) = 4$, $n = 500$, and $r = 5$. In each example, strictly lower triangular entries were generated according to the prior distribution, and diagonals were generated

by extracting diagonals from

$$D_1 \sim \text{diag}(W(d_1 + 2, \mathcal{D}_1)), \quad D_2 \sim \text{diag}(W(d_2 + 2, \mathcal{D}_2)) \quad (52)$$

$$\mathcal{D}_1 = \text{diag}(.75, 1, .2, .3, .1), \quad \mathcal{D}_2 = \text{diag}(1, .4, .3, .2) \quad (53)$$

According to the SCKPD Bayesian model, our first simulation example is performed under choice $k = 5$. In all the examples considered, $a_i^2 + a_i - \frac{\sqrt{F_D}}{d_i} \exp(-\gamma_D/(2d_1d_2)) = \epsilon$ was solved using the `nleqslv` package [14] in R, and each model was run using the supplemental computational results using `stan`'s `reduce sum` functionality for parallelization across the r^2 P-VL summands. The resulting posterior summarizations are found in Figure 1.

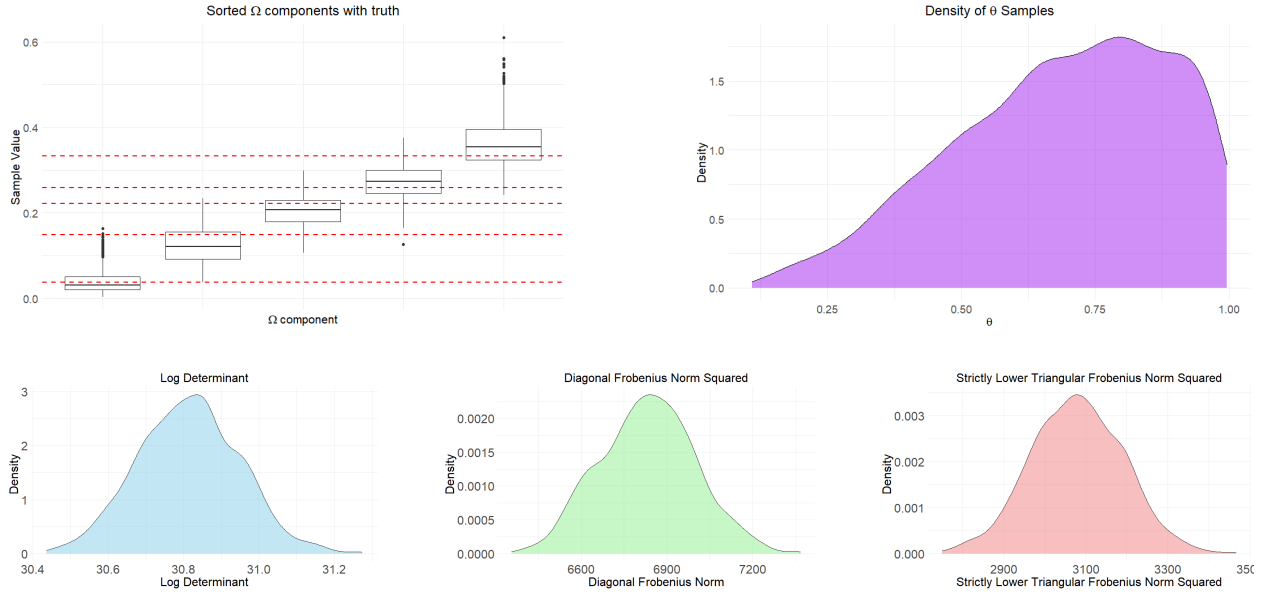


Figure 1: Posterior samples of the SCKPD model with $k = 5$, $r = 5$ with $d_1 = 4$, $d_2 = 5$. Top row: Ω components (left) with ground truth in dotted red line and θ (right). Bottom row: $\log |L^\dagger|$ (left), $\|\mathbb{D}(L^\dagger)\|_F^2$ (middle), $\|L^\dagger\|_F^2$ (right). Note the strong clustering of both the posterior samples of Ω and concentration of θ near 1.

In our second example, we modify the first data generation process to $r = 1$, leaving $k = 5$ to demonstrate the robust performance of the model to over-specification. The results of this posterior analysis are found in Figure 2.

We note that the global matrix statistics are robust to exact or over-specification due to the centering of the priors, as demonstrated in Figure 3.

Our third analysis focuses on the case of identifying true separability (i.e. the data generating

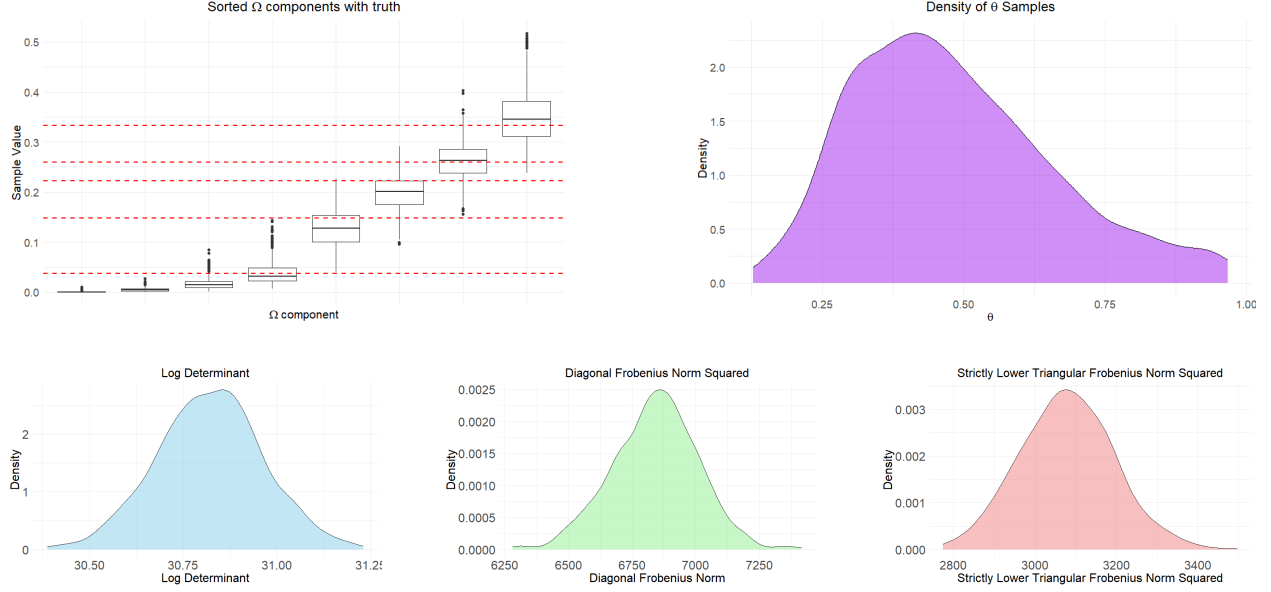


Figure 2: Posterior samples of the SCKPD model with $k = 8$, $r = 5$ with $d_1 = 4$, $d_2 = 5$. Top row: Ω components (left) with ground truth in dotted red line and θ (right). Bottom row: $\log |L^\dagger|$ (left), $\|\mathbb{D}(L^\dagger)\|_F^2$ (middle), $\|L^\dagger\|_F^2$ (right). Note the strong clustering of both the posterior samples of Ω and concentration of θ near 1.

process is focused on the case $R = 1$. In this case, we maintain the assumption $K = 5$ for overspecification, and evaluate the model's ability to recover only 1 non-zero component in Ω . The results of this analysis are shown in Figure 4.

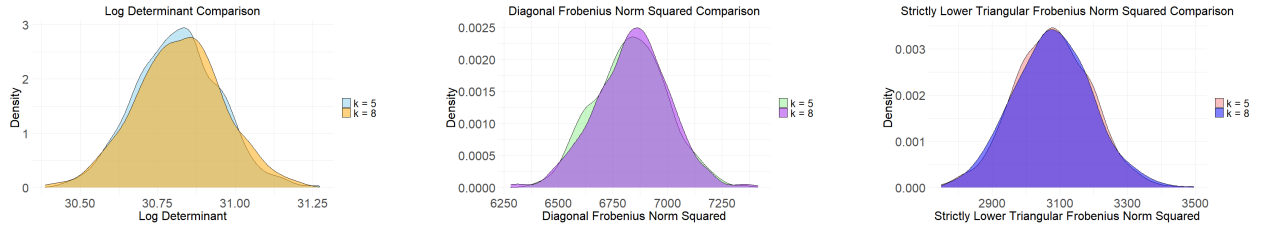


Figure 3: Comparison of posterior samples of the SCKPD model with $k = 5$ vs $k = 8$, and $r = 5$. From left to right: $\log |L^\dagger|$, $\|\mathbb{D}(L^\dagger)\|_F^2$, and $\|L^\dagger\|_F^2$.

In our third example, we modify the first data-generating process to $r = 1$, leaving $k = 5$ to illustrate the model's ability to detect true separability. We do not show global matrix statistics in this figure, as we are not comparing posterior consistency between different configurations in this setting, but rather a different data generating process. These results are found in Figure 4.

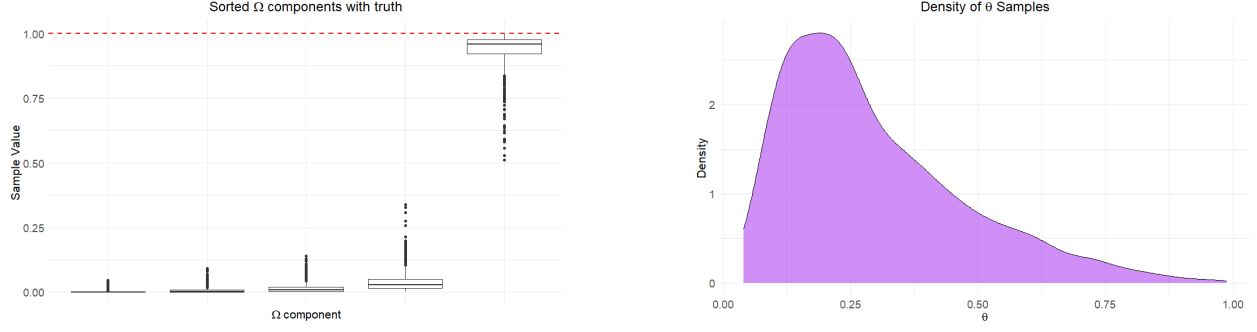


Figure 4: Posterior samples of the SCKPD model with $k = 5$, $r = 1$ with $d_1 = 4$, $d_2 = 5$. Ω components (left) with ground truth in dotted red line and θ (right). Note the strong clustering of both the posterior samples of $\Omega_{(5)}$ near 1 and concentration of θ near 0.

5.2 Seasonally Dynamic Covariance

In this section we will apply the SD-SCKPD model of Section (3.3) to an example where seasonal correlations are generated from a finite number of K Cholesky factors:

$$\begin{aligned}\Theta(t) &= L_t^\dagger [L_t^\dagger]^T \\ [L_1^{(i)}] &\stackrel{D}{=} [L_2^{(i)}] | \Omega, \beta, F_D, F_L \sim N(0, \sigma^2 = \omega_i(t)\beta) \\ \Omega(t+1) &= A\Omega(t)\end{aligned}$$

where $A \in \mathbb{R}_+^{K \times K}$ is a non-negative column-stochastic matrix:

$$\begin{aligned}A_{i,j} &\geq 0 \quad \forall i, j \\ \sum_{j=1}^K A_{i,j} &= 1 \quad \forall i.\end{aligned}$$

In this simulation example, we chose $d_1 = 5$, $d_2 = 2$, with $k = 5$, $r = 5$, with $n = 500$ per seasonal setting per cycle, and the columns of A were simulated according to

$$A[:, i] \sim \mathcal{D}(.05).$$

The results of the dynamic covariance model can be found in Figure 5.

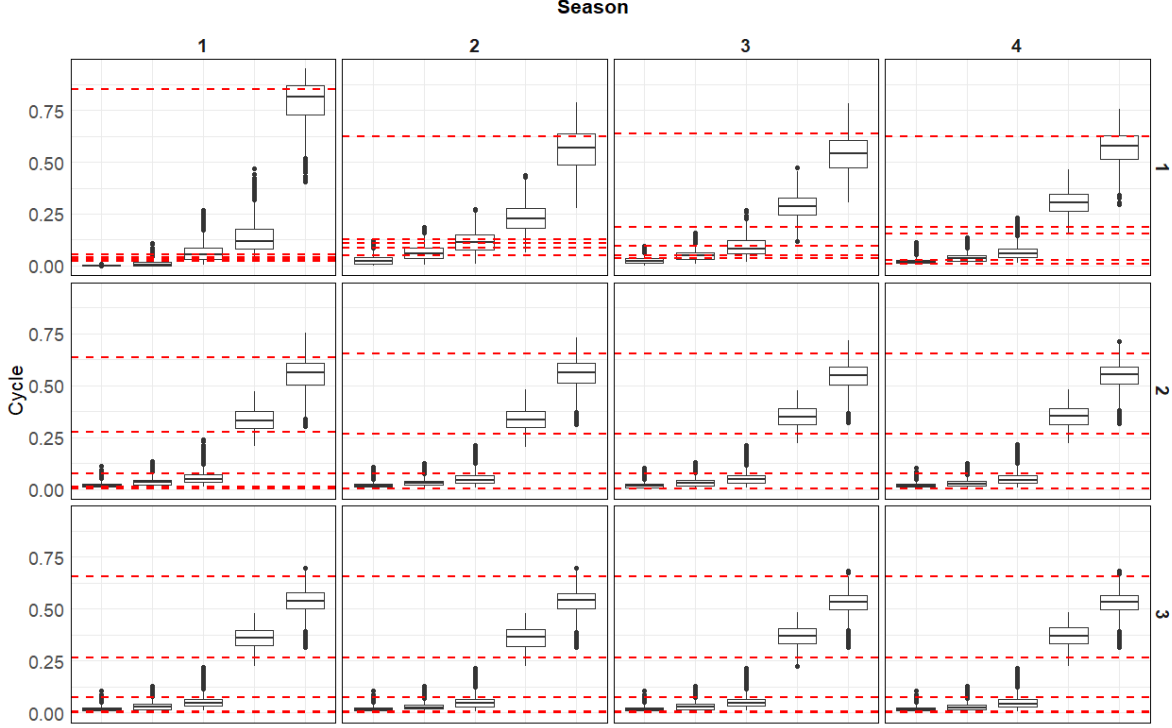


Figure 5: Ordered posterior samples of $\Omega(c, s)$ for seasonally changing Covariance. Seasonal changes are ordered across columns, cycle changes across rows. Horizontal red lines signify ground truth $\Omega_{c,s}$ at cycle c , season s , $c \in \{1, 2, 3\}$, $s \in \{1, 2, 3, 4\}$. Note the model can correctly detect regime shifts within a 95% credible interval while maintaining an appropriate sparsity level of $\Omega_{(1)}(c, s)$ and $\Omega_{(2)}(c, s)$. Moreover, the posterior adequately reflects the convergence of the steady-state distribution of the true $\Omega(c, s)$.

6 Real Data Examples

6.1 Wisconsin Breast Cancer

In this section we provide a Bayesian analysis for the degree of data precision matrix separability for the Wisconsin Breast Cancer dataset [1] using the model from Section 3.2. In particular, the Wisconsin Breast Cancer dataset is comprised of measurements of breast cancer cell nuclei derived from images using fine needle aspiration of breast mass. Statistics of {Mean, Standard Error, Worst} are computed for the features {Radius, Texture, Perimeter, Area, Smoothness, Compactness, Concavity, Number of Concave Points, Symmetry, Fractal Dimension}. For our analysis, we focus on the subset of characteristic statistics {Mean, Worst}, and features {Radius, texture, concavity, symmetry, fractal dimension} of malignant tumors. In total, this yields 212 matrix observations $\mathbf{Y}_1, \dots, \mathbf{Y}_{212} \in \mathbb{R}^{2 \times 5}$.

We assume the SCKPD Bayesian model for the precision matrix:

$$\begin{aligned} \text{vec}(\mathbf{Y}_1), \dots, \text{vec}(\mathbf{Y}_{567}) &\sim N(\bar{\mathbf{Y}}, \Theta = L^\dagger [L^\dagger]^T) \\ L^\dagger | \{L_1^{(i)}, L_2^{(i)}\}, \Omega &\sim \text{SCKPD}(\{L_1^{(i)}, L_2^{(i)}\}, \Omega), \quad L_1^{(i)} \in \mathcal{L}^+(5), L_2^{(i)} \in \mathcal{L}^+(2). \end{aligned}$$

If separability were true, by P-VL, then the degree of separability is upper bounded by 4, which we assume for K in our analysis. The results of this analysis are found in Figure 6.

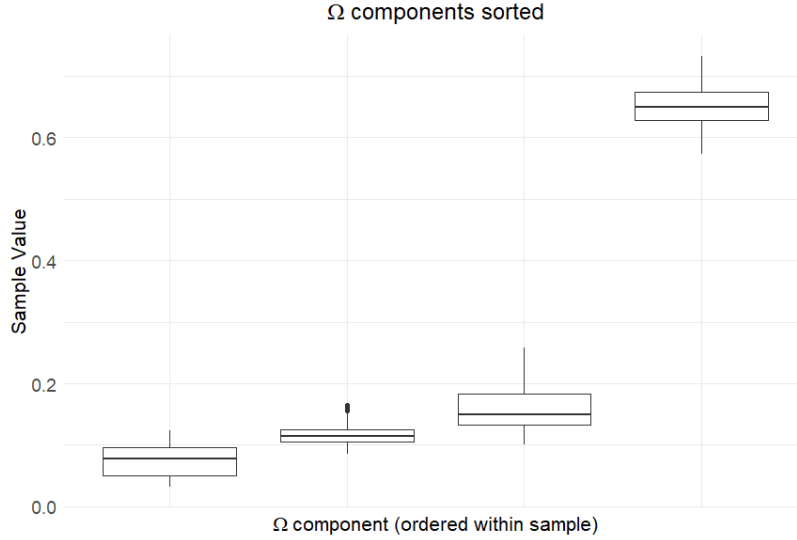


Figure 6: Sorted posterior Ω components under the SCKPD-B model for the analysis of the Wisconsin breast cancer dataset. Note all 4 components are non-zero, indicating a lack of separability in the precision matrix.

6.2 Continental United States Climate Analysis

In this section we apply the results of Section 3.3 to a Bayesian regression analysis of climate data in the continental United States. The data set consists of 48 cities in the continental United States, and our analysis focuses on the multivariate observations **TMAX**, **TMIN**, which are respectively the maximum and minimum ground temperature observations in tenths of degrees Celsius collected between spring 2020 and winter 2023.

We focus our analysis on inference of the covariance of the coefficients corresponding to periodic trends across the different cities. Specifically, we fit the following univariate OLS model indepen-

| | | | | | | | | |
|--------------------|----------------------|----------------------|--------------------|--------------------|--------------------|-------------------|-------------------|-------------------|
| $\alpha_{\cdot,1}$ | $\gamma_{1,\cdot,1}$ | $\gamma_{2,\cdot,1}$ | $\phi_{1,\cdot,1}$ | $\phi_{2,\cdot,1}$ | $\phi_{3,\cdot,1}$ | $\xi_{1,\cdot,1}$ | $\xi_{2,\cdot,1}$ | $\xi_{3,\cdot,1}$ |
| .47 | 1 | 1 | 1 | .55 | .62 | 1.00 | .85 | .13 |

| | | | | | | | | |
|--------------------|----------------------|----------------------|--------------------|--------------------|--------------------|-------------------|-------------------|-------------------|
| $\alpha_{\cdot,2}$ | $\gamma_{1,\cdot,2}$ | $\gamma_{2,\cdot,2}$ | $\phi_{1,\cdot,2}$ | $\phi_{2,\cdot,2}$ | $\phi_{3,\cdot,2}$ | $\xi_{1,\cdot,2}$ | $\xi_{2,\cdot,2}$ | $\xi_{3,\cdot,2}$ |
| 1 | 1 | 1 | .64 | .7 | .17 | 1 | .68 | .49 |

Table 1: Proportion of significance for OLS fits of equation (54) across the 48 datasets for TMIN (top row) and TMAX (bottom row). Note the significance of coefficients for annual cyclic patterns for both variables.

dently to each of the 48 cities where the output is $\hat{Y}_{c,t,1} = \hat{T}_{c,t,max}$, $\hat{Y}_{c,t,2} = \hat{T}_{c,t,min}$. Specifically:

$$\hat{Y}_{c,t,i} = \alpha_{c,i} + \sum_{j=1}^3 (\phi_{j,c,i} Y_{c,t-j,1} + \xi_{j,c,i} Y_{c,t-j,2}) + \gamma_{1,c,i} \sin\left(2\pi \frac{\Xi(t)}{365}\right) + \gamma_{2,c,i} \cos\left(2\pi \frac{\Xi(t)}{365}\right) + \epsilon \quad (54)$$

that is, we fit OLS models on a city-dependent intercept, AR(3) components with lags on $\hat{T}_{c,t,max}$ and $\hat{T}_{c,t,min}$, and annual periodic patterns, where $\frac{\Xi(t)}{365}$ denotes the fraction of time that has occurred within the season at that point. For example, assuming exactly 365 observations occurred for each year, $\frac{\Xi(500)}{365} = \frac{500-365}{365} = \frac{135}{365}$, indicating that observation 500 occurs at $\frac{135}{365}$ the first part of year 2.

For these separate OLS models, we achieved a mean R-squared of .884 and .831 and a mean standard error of 28.8 and 37.8 for tenths of degree Celsius for T_{min} and T_{max} , respectively. Table (1) below illustrates the proportion of models that were significant ($\mathbb{P}(\theta > |t|) < .05$).

As our analysis is focused specifically on the covariance of the coefficients for annual cyclic trends, we begin our analysis by evaluating the validity of our prior assumptions. In Figure (7), we fit the OLS model (54) across all season and year pairs, and compute $\mu(f(\hat{\Sigma}_{\gamma,s,y})) + 2\sigma(f(\hat{\Sigma}_{\gamma,s,y}))$, which are computed respectively across $s \in \{Spring, Summer, Fall, Winter\}$ and $y \in \{2020, 2021, 2022, 2023\}$. Note that this prior validation loses some model interpretability of annual cyclic trends but provides valuable insights into the individual correlation patterns of the resulting sample covariance matrix of γ across seasons. From the resulting covariance pattern, we can deduce that $tr(\Sigma_{\gamma,s,y})$ and $\log|\Sigma_{\gamma,s,y}|$ are approximately fixed over time.

From the full OLS model in (54), we propose the following Bayesian joint model with a random



Figure 7: Log determinant (left) and trace (right) of $\hat{\Sigma}_\gamma$ by season and year. Black dotted lines highlight the interval $\mu(f(\hat{\Sigma}_{\gamma,s,y})) + 2\sigma(f(\hat{\Sigma}_{\gamma,s,y}))$, where $f(\cdot)$ denotes correspondingly trace or log determinant. Points in red fall within the 2 sd interval, blue points are outliers for this region.

effects coefficient for the annual cyclic patterns:

$$\begin{aligned}\hat{Y}_{c,t,i} &= \alpha_{c,i} + \sum_{j=1}^3 (\phi_{j,i} Y_{c,t-j,1} + \xi_{j,i} Y_{c,t-j,2}) \\ &\quad + \gamma_{1,i} \sin\left(2\pi \frac{\Xi(t)}{365}\right) + \gamma_{2,i} \cos\left(2\pi \frac{\Xi(t)}{365}\right) + \epsilon_c \\ \alpha_{c,i} &\sim N(0, \sigma_\alpha) \\ \phi_{j,1}, \phi_{j,2} &\sim N(0, \sigma_\phi) \\ \xi_{j,1}, \xi_{j,2} &\sim N(0, \sigma_\xi) \\ \gamma &\sim N(\mu, \Sigma) \\ \mu &\sim N(0, \sigma_\mu) \\ \epsilon_c &\sim N^+(0, \sigma_\epsilon).\end{aligned}$$

In Table 2, we give a comparative analysis of the residual to the mean for 3 models in the 48 cities:

- Model 1: `auto.arima`, regressing T_{MAX} and T_{MIN} only on its own previous lags.
- Model 2: anisotropic diagonal covariance on γ ($\Sigma = \text{diag}(\tau_1, \tau_2, \tau_3, \tau_4)$, $\tau \stackrel{iid}{\sim} C^+(0, 1)$).
- Model 3: A dynamic case where Σ_s is parameterized according to L_t^\dagger of Section 3.3 with $K = 4$, where two column stochastic matrix parameters A_1, A_2 are introduced to account for assumed regime shifts between Spring 2021 and Summer 2021 ($A_1, s \in \{5, 6\}$) and a separate regime shift from Fall 2021 onward ($A_2, s \geq 7$).

For simplicity, we assume $\sigma_\phi = \sigma_\xi = 1$, $\sigma_\alpha = \sigma_\mu = \sigma_\epsilon = 5$ in each model. For each Bayesian model, the Bayesian R-squared ([10]) was not worse than the mean R-squared for independent OLS models.

| Model | $\mu(r_{TMIN})$ | $\sigma(r_{TMIN})$ | $IQR(r_{TMIN})$ | $\mu(r_{TMAX})$ | $\sigma(r_{TMAX})$ | $IQR(r_{TMAX})$ |
|-------|-----------------|--------------------|-----------------|-----------------|--------------------|-----------------|
| 1 | .294 | 31.8 | 37.8 | .303 | 39.4 | 45.6 |
| 2 | -.0771 | 29.6 | 35.3 | .551 | 39.1 | 46.0 |
| 3 | -.0696 | 29.5 | 35.2 | .241 | 39.1 | 46.4 |

Table 2: Summary Statistics of Residuals to Posterior Mean ($r = Y - (\mu|Y)$). Columns are ordered across cities according to: mean residual, mean standard deviation of residual, mean IQR of residual for TMIN (first 3 columns) and TMAX (last 3 columns), respectively. Note that in all but $IQR(r_{TMAX})$, the seasonally dynamic model for γ . outperformed all other models.

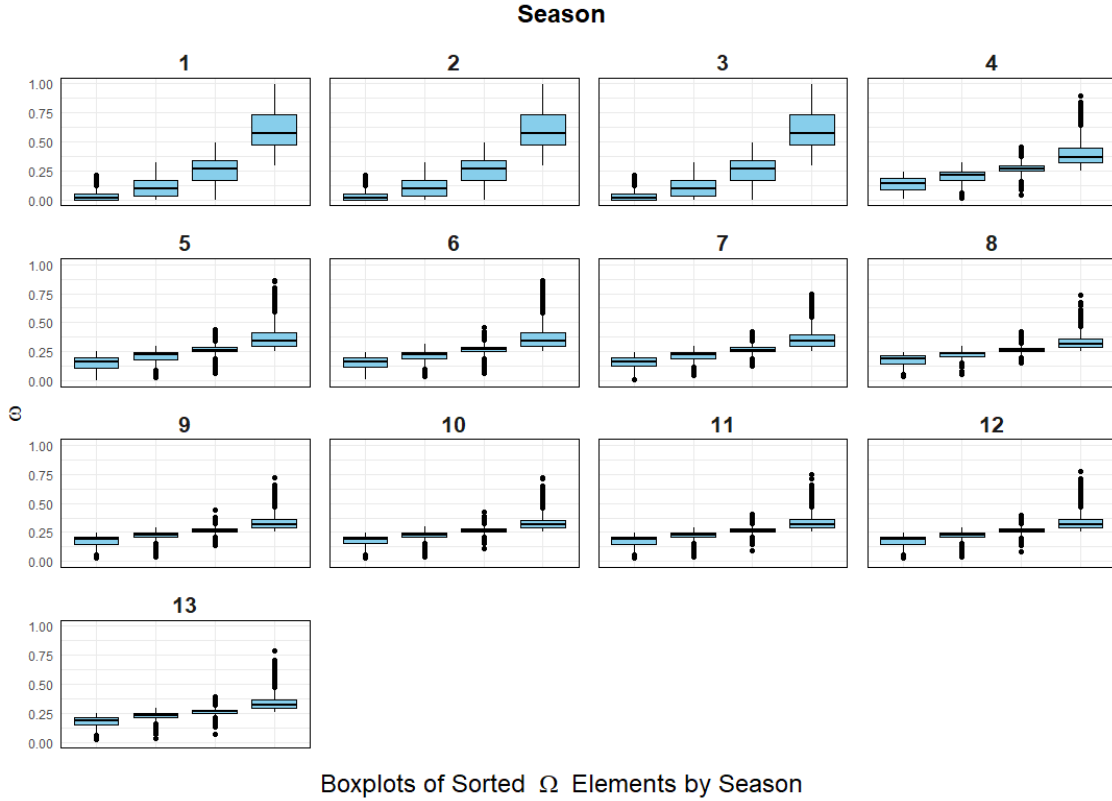


Figure 8: Sorted posterior Ω components under the SD-SCKPD model for γ within our regression model. Note the stabilization of the regime shift at \sim season 6, implicating a non-substantial regime shift for seasons $s \geq 7$.

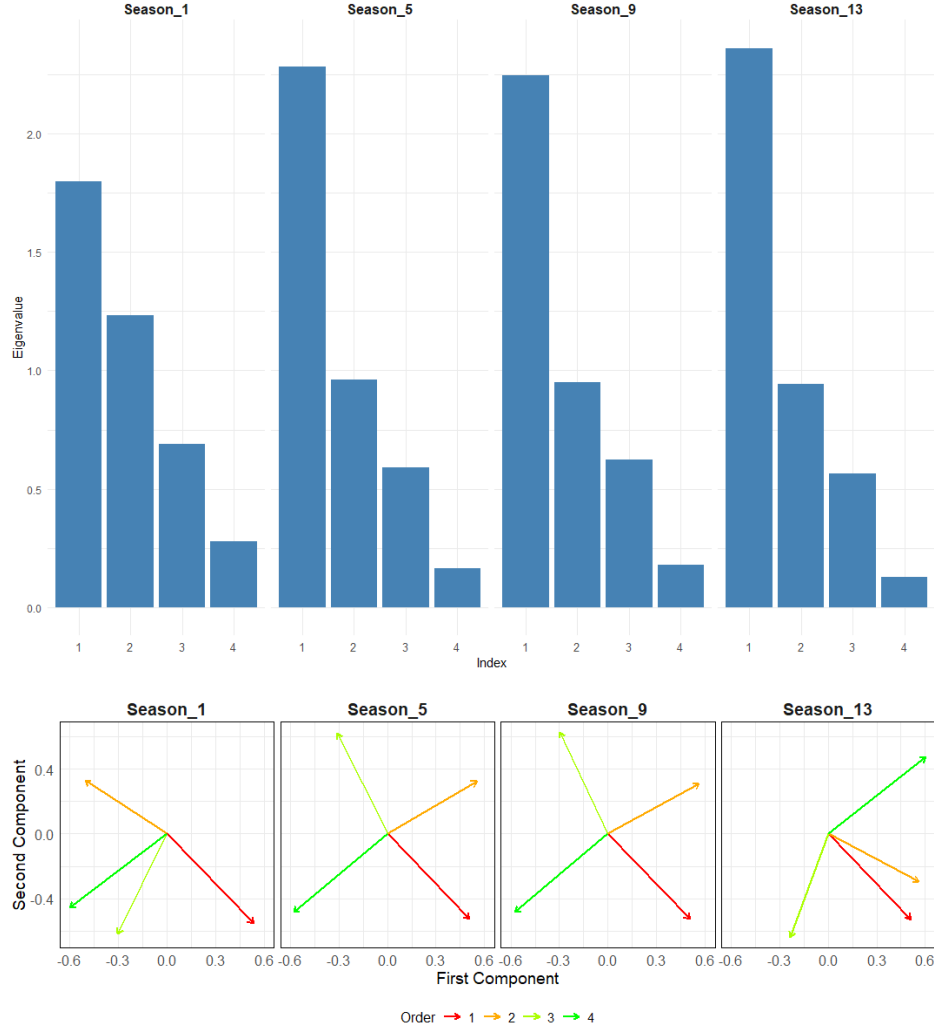


Figure 9: Eigenvalues (top row) and eigenvectors (bottom row) of the resulting Correlation matrices $\text{corr}(L_t L_t^T)$ for seasons 1, 5, 9, and 13. Performing a Procrustes analysis on the resulting eigenvectors between seasons 1 and all other seasons resulted in a maximal Procrustes sum of squares of $\approx 10^{-15}$ with a scaling of 1 and negligible translation. Hence, the eigenvectors themselves were all rotated versions of the resulting eigenvectors from season 1, but the changing eigenvalue structure then implies non-negligible seasonal evolution of the correlation matrix with respect to the significance of principal directions.

7 Conclusion

In this article, we explore the utility of a geometrically informed parameterization of Cholesky factors to relax the constraints imposed on the covariance of a tensor normal distribution. One potential avenue for future work is to consider a geodesic sampling approach. We noted that the posterior for this problem is indeed not geodesically convex. However, given the flexibility

permitted for posterior distributions on the Cholesky factor, it may be interesting to consider such a sampling approach when the corresponding posterior is poorly conditioned. In such a case, it would be beneficial to consider further modifications, such as parallel tempering, to alleviate the nonconvexity of such an approach. If such an approach were considered, relatively few modifications would need to be made. In particular, the Lebesgue measure for posterior distributions defined in the Riemannian manifold is insufficient for posterior sampling [4]. Instead, we need to resort to the Hausdorff measure according to the area formula [7]:

$$\mathcal{H}(dL|y) = \sqrt{|G(L)|}P(L|y)\lambda(dL)$$

where $\lambda(\cdot)$ refers to the Lebesgue measure and $G(\cdot)$ is the matrix metric tensor. Note that in the product manifold geometry, $G(L)$ is particularly simple to compute in closed form. Assuming our position is specified in vector form as:

$$vec(L) = (vec(\mathbb{D}(L)), vec(\lfloor L \rfloor))^t$$

then for the norm

$$\|V\|_L = \langle V, V \rangle_F + tr(\mathbb{D}(L)^{-1}\mathbb{D}(V)\mathbb{D}(L)^{-1}\mathbb{D}(V)) = V^T G(L) V.$$

Gives the metric tensor in matrix form as:

$$G(L) = \begin{pmatrix} \mathbb{D}(L)^{-1} \otimes \mathbb{D}(L)^{-1} & 0 \\ 0 & I_{\frac{d(d-1)}{2}} \end{pmatrix}$$

which simply gives $|G(L)| = |\mathbb{D}(L)|^2$. Then the use of geodesic Monte Carlo algorithms a geodesic approach would be efficient in regards to only requiring inversion of diagonal matrices.

Alternatively, exploring other metrics directly on SPD space could be worthwhile; the Cholesky parameterization explored here, while computationally tractable, yields cumbersome analytic gradients. With an SPD-valued metric, tractable gradients for the trace term were explored in [27], which is parallelizable within a geodesic Monte Carlo implementation. We show that the log-

Euclidean metric directly yields Fréchet means, which are multiway. Empirically, we found that the affine-invariant metric yields similar results. An alternative metric that we did not investigate was the Bures-Wasserstein metric [2], which takes the form:

$$g_{\Sigma}^{BW}(U, V) = \frac{1}{2} \text{tr}(\mathcal{L}_{\Sigma}[U]V)$$

where $\mathcal{L}_{\Sigma}[U]$ denotes the Lyapunov operator, or the solution to the system of equations:

$$\mathcal{L}_{\Sigma}[U]\Sigma + \Sigma\mathcal{L}_{\Sigma}[U] = U.$$

For $A, B \in \mathcal{P}^+(d)$, the corresponding geodesic distance is given by:

$$d^{BW}(A, B) = [\text{tr}(A) + \text{tr}(B) - 2\text{tr}(A^{\frac{1}{2}}BA^{\frac{1}{2}})^{\frac{1}{2}}]^{\frac{1}{2}}.$$

To our knowledge, no closed form exists for the Fréchet mean of such a distance, and in such a case may be an interesting avenue for investigating differentiation directly through the argmin operator, as was explored in [24]. However, we note that the matrix metric is given by [13] as

$$G_{BW}(\Sigma) = \Sigma \oplus \Sigma$$

where \oplus denotes the Kronecker sum operator:

$$A \oplus B = A \otimes I + I \otimes B$$

where an obvious difficulty with this then being the calculation of the corresponding Hausdorff measure due to the intractability of the determinant of the metric.

A clear modification to the model assumption on L^{\dagger} is to remove the assumed multiway structure on the diagonal. That is, instead model L^{\dagger} as:

$$L^{\dagger} = \sum_{i=1}^K [L_1^{(i)} \otimes L_2^{(i)}] + \exp(D)$$

for an unconstrained diagonal matrix D . While limiting in its ability to detect true separability of

a resulting covariance matrix, it provides an obvious generalization in flexibility at little increased computational complexity of the model. However, we note that many of the computational results regarding representation of the likelihood under the P-VL and the time-varying matrix normally distributed regression parameters techniques discussed in the supplement may require substantial modifications.

Lastly, this article has thus far made no mention of relationships to spatial approximations, where separability is a common assumption. When combined with the implications of how conditional independence in space-time models is well known to be driven by sparsity in the entries of Cholesky factors of precision or covariance matrices in such models through the Vecchia approximation [21], investigating methods for averaging over separable space-time functions could be a fruitful direction for investigation with respect to the scalability of the methods described in this article.

8 Supplementary Material

8.1 Static Covariance

In this section we consider several possible algebraic manipulations of the likelihood for efficient computation of the SCKPD Bayesian model.

We start by observing that if:

$$\Sigma^{-1} = LL^T$$

$$L = \sum_{i=1}^K [L_1^{(i)} \otimes L_2^{(i)}] + D_1 \otimes D_2.$$

Then first note that

$$\begin{aligned} LL^T &= \left[\sum_{k=1}^K [L_1^{(k)} \otimes L_2^{(k)}] + D_1 \otimes D_2 \right] \left[\sum_{k=1}^K [L_1^{(k)} \otimes L_2^{(k)}] + D_1 \otimes D_2 \right]^T \\ &= \sum_{k_1=1}^K \sum_{k_2=1}^K [L_1^{(k_1)} \otimes L_2^{(k_1)}] [L_1^{(k_2)} \otimes L_2^{(k_2)}]^T \\ &\quad + \sum_{k=1}^K [L_1^{(k)} \otimes L_2^{(k)}] D_1 \otimes D_2 + \sum_{k=1}^K [L_1^{(k)} \otimes L_2^{(k)}]^T D_1 \otimes D_2 \\ &\quad + D_1^2 \otimes D_2^2. \end{aligned}$$

Expanding the first term:

$$\begin{aligned} &[L_1^{(i)} \otimes L_2^{(i)}] [L_1^{(j)} \otimes L_2^{(j)}] \\ &= ([L_1^{(i)}] \otimes D_2 + D_1 \otimes [L_2^{(i)}] + D_1 \otimes D_2) ([L_1^{(j)}]^T \otimes D_2 + D_1 \otimes [L_2^{(j)}]^T + [L_1^{(j)}]^T \otimes [L_2^{(j)}]^T) \\ &= [L_1^{(i)}] [L_1^{(j)}]^T \otimes D_2^2 + [L_1^{(i)}] D_1 \otimes D_2 [L_2^{(j)}]^T + [L_1^{(i)}] [L_1^{(j)}]^T \otimes D_2 [L_2^{(j)}]^T \\ &\quad + D_1 [L_1^{(j)}]^T \otimes [L_2^{(i)}] D_2 + D_1^2 \otimes [L_2^{(i)}] [L_2^{(j)}]^T + D_1 [L_1^{(j)}]^T \otimes [L_2^{(i)}] [L_2^{(j)}]^T \\ &\quad + D_1 [L_1^{(j)}]^T \otimes D_2^2 + D_1^2 \otimes D_2 [L_2^{(j)}]^T + D_1 [L_1^{(j)}]^T \otimes D_2 [L_2^{(j)}]^T. \end{aligned}$$

Likewise the second term is expanded as:

$$[L_1^{(k)} \otimes L_2^{(k)}] D_1 \otimes D_2 = [L_1^{(k)}] D_1 \otimes D_2^2 + D_1^2 \otimes [L_2^{(k)}] D_2 + [L_1^{(k)}] D_1 \otimes [L_2^{(k)}] D_2$$

and third term is given by:

$$\lfloor L_1^{(k)} \otimes L_2^{(k)} \rfloor^T D_1 \otimes D_2 = \lfloor L_1^{(k)} \rfloor^T D_1 \otimes D_2^2 + D_1^2 \otimes \lfloor L_2^{(k)} \rfloor^T D_2 + \lfloor L_1^{(k)} \rfloor^T D_1 \otimes \lfloor L_2^{(k)} \rfloor^T D_2$$

$$\text{tr}(\Sigma^{-1} \sum_{i=1}^n y_i y_i^T) = \text{tr}(\left[\sum_{k=1}^K \lfloor L_1^{(k)} \otimes L_2^{(k)} \rfloor + D_1 \otimes D_2 \right] \left[\sum_{k=1}^K \lfloor L_1^{(k)} \otimes L_2^{(k)} \rfloor + D_1 \otimes D_2 \right]^T \sum_{i=1}^n y_i y_i^T).$$

It is clear that these computations quickly become computationally cumbersome for finding an analytic solution, where in total we will produce $K^2 + 2k + 1$ total summands, along with needing to construct $T^{(i)}(S, \cdot)$ for each term. As in the case of $D = 2$, we will instead take advantage of the P-VL decomposition in the same way as [28] to create a more compact form of the likelihood. Letting $\sum_{i=1}^N y_i y_i^T = \sum_{q=1}^{r^2} A_q \otimes B_q$, with $r = \min\{d_1, d_2\}$, direct calculation gives

$$\begin{aligned} L^T \sum_{i=1}^N y_i y_i^T &= \sum_{q=1}^{r^2} D_1 A_q \otimes D_2 B_q \\ &+ \left(\sum_{j=1}^K \lfloor L_1^{(j)} \rfloor^T A_q \otimes D_2 B_q + D_1 A_q \otimes \lfloor L_2^{(j)} \rfloor^T B_q + \lfloor L_1^{(j)} \rfloor^T A_q \otimes \lfloor L_2^{(j)} \rfloor^T B_q \right). \end{aligned}$$

From this, it is clear that

$$\begin{aligned}
LL^T \sum_{i=1}^N y_i y_i^T &= \sum_{q=1}^{r^2} [D_1^2 A_q \otimes D_2^2 B_q \\
&+ \left(\sum_{i=1}^K [L_1^{(i)}] D_1 A_q \otimes D_2^2 B_q + D_1^2 A_q \otimes [L_2^{(i)}] D_2 B_q + [L_1^{(i)}] D_1 A_q \otimes [L_2^{(i)}] D_2 B_q \right) \\
&+ \left(\sum_{j=1}^K D_1 [L_1^{(j)}]^T A_q \otimes D_2^2 B_q + D_1^2 A_q \otimes D_2 [L_2^{(j)}]^T B_q + D_1 [L_1^{(j)}]^T A_q \otimes D_2 [L_2^{(j)}]^T B_q \right) \\
&+ \sum_{i=1}^K \sum_{j=1}^K ([L_1^{(i)}] [L_1^{(j)}]^T A_q \otimes D_2^2 B_q + [L_1^{(i)}] D_1 A_q \otimes D_2 [L_2^{(j)}]^T B_q \\
&+ [L_1^{(i)}] [L_1^{(j)}]^T A_q \otimes [L_2^{(i)}] [L_2^{(j)}]^T B_q + D_1 [L_1^{(j)}]^T A_q \otimes [L_2^{(i)}] D_2 B_q \\
&+ D_1^2 A_q \otimes [L_2^{(i)}] [L_2^{(j)}]^T B_q + D_1 [L_1^{(j)}]^T A_q \otimes [L_2^{(i)}] [L_2^{(j)}]^T B_q \\
&+ [L_1^{(i)}] [L_1^{(j)}]^T A_q \otimes [L_2^{(i)}] D_2 B_q + [L_1^{(i)}] D_1 A_q \otimes [L_2^{(i)}] [L_2^{(j)}]^T B_q \\
&+ [L_1^{(i)}] [L_1^{(j)}]^T A_q \otimes [L_2^{(i)}] [L_2^{(j)}]^T B_q).
\end{aligned}$$

By linearity of the trace and leveraging two properties of Kronecker products:

$$(A \otimes B)(C \otimes D) = AC \otimes BD$$

$$\text{tr}(A \otimes B) = \text{tr}(A)\text{tr}(B)$$

the trace is then expressible as:

$$\begin{aligned}
tr(LL^T \sum_{i=1}^N y_i y_i^T) &= \sum_{q=1}^{r^2} [tr(D_1^2 A_q) tr(D_2^2 B_q) \\
&+ (\sum_{i=1}^K tr(\lfloor L_1^{(i)} \rfloor D_1 A_q) tr(D_2^2 B_q) + tr(D_1^2 A_q) tr(\lfloor L_2^{(i)} \rfloor D_2 B_q)) \\
&+ (\sum_{i=1}^K tr(\lfloor L_1^{(i)} \rfloor D_1 A_q) tr(\lfloor L_2^{(i)} \rfloor D_2 B_q)) \\
&+ (\sum_{j=1}^K tr(D_1 \lfloor L_1^{(j)} \rfloor^T A_q) tr(D_2^2 B_q) + tr(D_1^2 A_q) tr(D_2 \lfloor L_2^{(j)} \rfloor^T B_q) \\
&+ tr(D_1 \lfloor L_1^{(j)} \rfloor^T A_q) tr(D_2 \lfloor L_2^{(j)} \rfloor^T B_q)) \\
&+ \sum_{i=1}^K \sum_{j=1}^K (tr(\lfloor L_1^{(i)} \rfloor \lfloor L_1^{(j)} \rfloor^T A_q) tr(D_2^2 B_q) + tr(\lfloor L_1^{(i)} \rfloor D_1 A_q) tr(D_2 \lfloor L_2^{(j)} \rfloor^T B_q) \\
&+ tr(\lfloor L_1^{(i)} \rfloor \lfloor L_1^{(j)} \rfloor^T A_q) tr(\lfloor L_2^{(i)} \rfloor \lfloor L_2^{(j)} \rfloor^T B_q) + tr(D_1 \lfloor L_1^{(j)} \rfloor^T A_q) tr(\lfloor L_2^{(i)} \rfloor D_2 B_q) \\
&+ tr(D_1^2 A_q) tr(\lfloor L_2^{(i)} \rfloor \lfloor L_2^{(j)} \rfloor^T B_q) + tr(D_1 \lfloor L_1^{(j)} \rfloor^T A_q) tr(\lfloor L_2^{(i)} \rfloor \lfloor L_2^{(j)} \rfloor^T B_q) \\
&+ tr(\lfloor L_1^{(i)} \rfloor \lfloor L_1^{(j)} \rfloor^T A_q) tr(\lfloor L_2^{(i)} \rfloor D_2 B_q) + tr(\lfloor L_1^{(i)} \rfloor D_1 A_q) tr(\lfloor L_2^{(i)} \rfloor \lfloor L_2^{(j)} \rfloor^T B_q) \\
&+ tr(\lfloor L_1^{(i)} \rfloor \lfloor L_1^{(j)} \rfloor^T A_q) tr(\lfloor L_2^{(i)} \rfloor \lfloor L_2^{(j)} \rfloor^T B_q))].
\end{aligned}$$

While many summands are present within this, it's clear that each individual trace term is a sparse matrix multiplication. Moreover, we can leverage the fact that the P-VL decomposition inherits the following symmetry property

$$S = \sum_{i=1}^{r^2} A_i \otimes B_i, \quad S \in \mathcal{S}(d) \implies A_i, B_i \in \mathcal{S}(d_1) \times \mathcal{S}(d_2) \text{ for all } i.$$

Using the above property, and noting $(ABC)^T = C^T B^T A^T$, then observe

$$(\lfloor L_t^{(i)} \rfloor D_t C_q)^T = C_q D_t \lfloor L_t^{(i)} \rfloor^T.$$

Further, by invariance of trace under cyclic permutations and transpositions, it is evident that

$$\text{tr}(\lfloor L_t^{(i)} \rfloor D_t C_q) = \text{tr}(C_q D_t \lfloor L_t^{(i)} \rfloor^T) = \text{tr}(D_t \lfloor L_t^{(i)} \rfloor^T C_q).$$

Which gives an immediate simplification as:

$$\begin{aligned} & \left(\sum_{i=1}^K \text{tr}(\lfloor L_1^{(i)} \rfloor D_1 A_q) \text{tr}(D_2^2 B_q) + \text{tr}(D_1^2 A_q) \text{tr}(\lfloor L_2^{(i)} \rfloor D_2 B_q) + \text{tr}(\lfloor L_1^{(i)} \rfloor D_1 A_q) \text{tr}(\lfloor L_2^{(i)} \rfloor D_2 B_q) \right) \\ & + \left(\sum_{j=1}^K \text{tr}(D_1 \lfloor L_1^{(j)} \rfloor^T A_q) \text{tr}(D_2^2 B_q) + \text{tr}(D_1^2 A_q) \text{tr}(D_2 \lfloor L_2^{(j)} \rfloor^T B_q) \right. \\ & \left. + \text{tr}(D_1 \lfloor L_1^{(j)} \rfloor^T A_q) \text{tr}(D_2 \lfloor L_2^{(j)} \rfloor^T B_q) \right) \\ & = 2 \left(\sum_{i=1}^K \text{tr}(\lfloor L_1^{(i)} \rfloor D_1 A_q) \text{tr}(D_2^2 B_q) + \text{tr}(D_1^2 A_q) \text{tr}(\lfloor L_2^{(i)} \rfloor D_2 B_q) + \text{tr}(\lfloor L_1^{(i)} \rfloor D_1 A_q) \text{tr}(\lfloor L_2^{(i)} \rfloor D_2 B_q) \right). \end{aligned}$$

Now note that for the trace of a matrix product, we can write it in an order of complexity faster by leveraging the Hadamard product form

$$\text{tr}(AB) = \sum_i \sum_j (A^T \odot B)_{i,j} = \sum_i \sum_j A[j, i] B[i, j].$$

We will use $\sigma(A, B) = \sum_i \sum_j (A^T \odot B)_{i,j}$ to denote this less computationally taxing form. Then

we can rewrite $\text{tr}(LL^T \sum_{i=1}^N y_i y_i^T)$ as:

$$\begin{aligned}
\text{tr}(LL^T \sum_{i=1}^N y_i y_i^T) &= \sum_{q=1}^{r^2} [\sigma(D_1^2, A_q) \sigma(D_2^2, B_q) + \\
&\quad + 2 \sum_{i=1}^K \sigma(\lfloor L_1^{(i)} \rfloor, D_1 A_q) \sigma(D_2^2, B_q) + \sigma(D_1^2, A_q) \sigma(\lfloor L_2^{(i)} \rfloor, D_2 B_q) \\
&\quad + 2 \sum_{i=1}^K \sigma(\lfloor L_1^{(i)} \rfloor, D_1 A_q) \sigma(\lfloor L_2^{(i)} \rfloor, D_2 B_q) \\
&\quad + \sum_{i=1}^K \sum_{j=1}^K (\sigma(\lfloor L_1^{(i)} \rfloor, \lfloor L_1^{(j)} \rfloor^T A_q) \sigma(D_2^2, B_q) + \sigma(\lfloor L_1^{(i)} \rfloor, D_1 A_q) \sigma(D_2, \lfloor L_2^{(j)} \rfloor^T B_q) \\
&\quad + \sigma(\lfloor L_1^{(i)} \rfloor, \lfloor L_1^{(j)} \rfloor^T A_q) \sigma(\lfloor L_2^{(i)} \rfloor, \lfloor L_2^{(j)} \rfloor^T B_q) + \sigma(D_1, \lfloor L_1^{(j)} \rfloor^T A_q) \sigma(\lfloor L_2^{(i)} \rfloor, \lfloor L_2^{(j)} \rfloor^T B_q) \\
&\quad + \sigma(D_1^2, A_q) \sigma(\lfloor L_2^{(i)} \rfloor, \lfloor L_2^{(j)} \rfloor^T B_q) + \sigma(D_1, \lfloor L_1^{(j)} \rfloor^T A_q) \sigma(\lfloor L_2^{(i)} \rfloor, \lfloor L_2^{(j)} \rfloor^T B_q) \\
&\quad + \sigma(\lfloor L_1^{(i)} \rfloor, \lfloor L_1^{(j)} \rfloor^T A_q) \sigma(\lfloor L_2^{(i)} \rfloor, D_2 B_q) + \sigma(\lfloor L_1^{(i)} \rfloor, D_1 A_q) \sigma(\lfloor L_2^{(i)} \rfloor, \lfloor L_2^{(j)} \rfloor^T B_q) \\
&\quad + \sigma(\lfloor L_1^{(i)} \rfloor, \lfloor L_1^{(j)} \rfloor^T A_q) \sigma(\lfloor L_2^{(i)} \rfloor, \lfloor L_2^{(j)} \rfloor^T B_q))].
\end{aligned}$$

Observe that each summand is then a Hadamard product between a sparse matrix and a matrix resulting from a sparse multiplication.

Note that for the seasonally dynamic covariance model of Section 3.3, no significant modifications need be made to the results from this section beyond replacing $\{L_1^{(i)}, L_2^{(i)}\}_{i=1}^K$ with it's seasonal/cyclic counterparts $\{L_{1,(c,s)}^{(i)}, L_{2,(c,s)}^{(i)}\}$ which respectively act on $\{A_q^{(c,s)}, B_q^{(c,s)}\}_{q=1}^{r^2}$. Note this latter point simply involves for a given collection of observations $\{y_1^{(c,s)}, \dots, y_N^{(c,s)}\}$ belonging to season s , cycle c and performing the decomposition

$$\sum_{i=1}^N y_i^{(c,s)} (y_i^{(c,s)})^T = \sum_{i=1}^{r^2} A_i^{(c,s)} \otimes B_i^{(c,s)}$$

8.2 Seasonally Varying Parameterization

In this section we deal with the situation of a time varying mean. In particular, we assume the case of Section 6.2, where

$$Y_t \sim N(\beta X, \sigma^2 I) \quad (55)$$

$$\beta_S \sim N((\bar{\beta}_{-S}, \bar{\beta}_S), \Sigma) \quad (56)$$

for some subset $\beta_S \subseteq \beta$, and

$$\Sigma = \begin{pmatrix} \tau^2 I_d & \mathbf{0} \\ \mathbf{0} & L^\dagger L^{\dagger T} \end{pmatrix}$$

Note that this can be a particularly efficient form compared to the data covariance case. Reparameterization trick can be used in two ways for this form. The less efficient but more direct way is through matrix-vector multiplication as:

$$\text{vec}(\beta) \sim (\tau x_1, L^\dagger x_2) + \text{vec}(\bar{\beta})$$

where x_1, x_2 are independently distributed as $x_1, x_2 \sim N(0, I)$. However, note that the inefficiency of this is then attributed to the necessity of explicit computation of the Kronecker product for the strictly lower triangular entries for each $i \in \{1, \dots, K\}$. The efficient representation of distributed computing from the previous section is infeasible, as it would require the iterative P-VL decomposition of the matricization of x_2 at each iteration.

Instead, a more appealing form would come from the matrix normal form. This can be viewed directly from the matricization and vectorization:

Definition 8.1. Let $v \in \mathbb{R}^{d_1 d_2}$, and define the **mode-i folding** of v , $\mathcal{F}_{(i)}(v) = V_{(i)} \in \mathbb{R}^{d_i \times d_{-i}}$ element-wise as:

$$[V_{(i)}]_{p,q} = v_{(p-1)d_i + q}$$

Define the **mode-i unfolding** as the corresponding reverse mapping $\mathcal{UF}_{(i)}(V_{(i)}) \rightarrow v$

From these definitions, in the case $D = 2$, for $x \in \mathbb{R}^{d_1 d_2}$ such that $x \sim N(0, I)$, then $X_{(1)} = \mathcal{F}_{(1)}(x) \sim MN(0, I, I)$. Observing that the corresponding folding operation is a linear operator, it

can easily be seen that:

$$\begin{aligned}
L^\dagger x &= \left[\sum_{i=1}^K \mathbb{D}(L_1^{(i)}) \otimes \lfloor L_2^{(i)} \rfloor + \lfloor L_1^{(i)} \rfloor \otimes \mathbb{D}(L_2) + \lfloor L_1^{(i)} \rfloor \otimes \lfloor L_2^{(i)} \rfloor + D_1 \otimes D_2 \right] x \\
\implies \mathcal{F}_{(1)}(L^\dagger x) &= D_2 F_{(1)}(x) D_1 \\
&\quad + \sum_{i=1}^K \lfloor L_2^{(i)} \rfloor X_{(1)} D_1 + D_2 X_{(1)} \lfloor L_1^{(i)} \rfloor + \lfloor L_2^{(i)} \rfloor X_{(1)} \lfloor L_1^{(i)} \rfloor \\
\implies L^\dagger x &= \mathcal{UF}_{(1)}(\mathcal{F}_{(1)}(L^\dagger x)) = \mathcal{UF}_{(1)}(D_2 X_{(1)} D_1) \\
&\quad + \sum_{i=1}^K \mathcal{UF}_{(1)}(\lfloor L_2^{(i)} \rfloor X_{(1)} D_1) + \mathcal{UF}_{(1)}(D_2 X_{(1)} \lfloor L_1^{(i)} \rfloor) + \mathcal{UF}_{(1)}(\lfloor L_2^{(i)} \rfloor X_{(1)} \lfloor L_1^{(i)} \rfloor).
\end{aligned}$$

Note this form is much more efficient than through the use of P-VL, as gradient complexity no longer scales multiplicatively with $n > 1$ observations.

Funding: This research was partially supported by a grant from New Presbyterian Hospital and the National Institute of Allergy and Infectious Diseases of the National Institutes of Health under award number P01AI159402.

References

- [1] Abien Fred M Agarap. On breast cancer detection: an application of machine learning algorithms on the Wisconsin diagnostic dataset. In *Proceedings of the 2nd International Conference on Machine Learning and Soft Computing*, pages 5–9, 2018. [32](#)
- [2] Rajendra Bhatia, Tanvi Jain, and Yongdo Lim. On the bures–wasserstein distance between positive definite matrices. *Expositiones Mathematicae*, 37(2):165–191, 2019. [39](#)
- [3] Patrick E Brown, Gareth O Roberts, Kjetil F K  resen, and Stefano Tonellato. Blur-generated non-separable space–time models. *Journal of the Royal Statistical Society Series B: Statistical Methodology*, 62(4):847–860, 2000. [2](#)
- [4] Simon Byrne and Mark Girolami. Geodesic monte carlo on embedded manifolds. *Scandinavian Journal of Statistics*, 40(4):825–845, 2013. [25](#), [38](#)
- [5] Wanfang Chen, Marc G Genton, and Ying Sun. Space-time covariance structures and models. *Annual Review of Statistics and Its Application*, 8(1):191–215, 2021. [2](#)
- [6] Luc Devroye. Nonuniform random variate generation. *Handbooks in Operations Research and Management Science*, 13:83–121, 2006. [28](#)
- [7] Herbert Federer. *Geometric Measure Theory*. Springer, 2014. [38](#)
- [8] Bailey K Fosdick and Peter D Hoff. Separable factor analysis with applications to mortality data. *The Annals of Applied Statistics*, 8(1):120, 2014. [2](#)
- [9] Alan E Gelfand. Gibbs sampling. *Journal of the American Statistical Association*, 95(452):1300–1304, 2000. [4](#) [2](#)
- [10] Andrew Gelman, Ben Goodrich, Jonah Gabry, and Aki Vehtari. R-squared for Bayesian regression models. *The American Statistician*, 2019. [36](#)

- [11] Marc G Genton. Separable approximations of space-time covariance matrices. *Environmetrics: The Official Journal of the International Environmetrics Society*, 18(7):681–695, 2007. 2
- [12] Brian C Hall and Brian C Hall. *Lie Groups, Lie Algebras, and Representations*. Springer, 2013. 11
- [13] Andi Han, Bamdev Mishra, Pratik Kumar Jawanpuria, and Junbin Gao. On riemannian optimization over positive definite matrices with the bures-wasserstein geometry. *Advances in Neural Information Processing Systems*, 34:8940–8953, 2021. 39
- [14] Berend Hasselman and Maintainer Berend Hasselman. Package ‘nleqslv’. *R package version*, 3(2), 2018. 29
- [15] Laura A Hatfield and Alan M Zaslavsky. Separable covariance models for health care quality measures across years and topics. *Statistics in Medicine*, 37(12):2053–2066, 2018. 2
- [16] Frank L Hitchcock. The expression of a tensor or a polyadic as a sum of products. *Journal of Mathematics and Physics*, 6(1-4):164–189, 1927. 6
- [17] Helmut Hofer and Eduard Zehnder. *Symplectic Invariants and Hamiltonian Dynamics*. Birkhäuser, 2012. 5
- [18] Peter D Hoff. Separable covariance arrays via the tucker product, with applications to multi-variate relational data. *Bayesian Analysis*, 2011. 2, 6, 16
- [19] Andrew Holbrook, Shiwei Lan, Alexander Vandenberg-Rodes, and Babak Shahbaba. Geodesic lagrangian monte carlo over the space of positive definite matrices: with application to Bayesian spectral density estimation. *Journal of Statistical Computation and Simulation*, 88(5):982–1002, 2018. 25
- [20] Piet Hut, Jun Makino, and Steve McMillan. Building a better leapfrog. *Astrophysical Journal, Part 2-Letters (ISSN 0004-637X)*, vol. 443, no. 2, p. L93-L96, 443:L93–L96, 1995. 5
- [21] Matthias Katzfuss and Joseph Guinness. A general framework for vecchia approximations of gaussian processes. *Statistical Science*, 36(1):124–141, 2021. 40

- [22] Tamara Gibson Kolda. Multilinear operators for higher-order decompositions. Technical report, Sandia National Laboratories (SNL), Albuquerque, NM, and Livermore, CA, 2006. [7](#)
- [23] Zhenhua Lin. Riemannian geometry of symmetric positive definite matrices via cholesky decomposition. *SIAM Journal on Matrix Analysis and Applications*, 40(4):1353–1370, 2019. [3](#), [9](#), [12](#), [26](#)
- [24] Aaron Lou, Isay Katsman, Qingxuan Jiang, Serge Belongie, Ser-Nam Lim, and Christopher De Sa. Differentiating through the fréchet mean. In *International Conference on Machine Learning*, pages 6393–6403. PMLR, 2020. [39](#)
- [25] Radford M Neal et al. Mcmc using hamiltonian dynamics. *Handbook of Markov Chain Monte Carlo*, 2(11):2, 2011. [3](#), [5](#)
- [26] N. P. Pitsanis. *The Kronecker product in approximation and fast transform generation*. PhD thesis, Cornell University, Ithaca, NY, 1997. [2](#), [15](#)
- [27] Quinn Simonis and Martin T. Wells. Geodesic variational Bayes for multiway covariances, 2025. [38](#)
- [28] Quinn Simonis and Martin T. Wells. Separable geodesic lagrangian monte carlo for inference in 2-way covariance models, 2025. [25](#), [42](#)
- [29] Dogyoon Song and Alfred O Hero. On separability of covariance in multiway data analysis. *arXiv preprint arXiv:2302.02415*, 2023. [2](#)
- [30] Theodoros Tsiligkaridis and Alfred O Hero. Covariance estimation in high dimensions via Kronecker product expansions. *IEEE Transactions on Signal Processing*, 61(21):5347–5360, 2013. [3](#)
- [31] Ledyard R Tucker. Some mathematical notes on three-mode factor analysis. *Psychometrika*, 31(3):279–311, 1966. [8](#)
- [32] Saiteja Utpala, Praneeth Vepakomma, and Nina Miolane. Differentially private fréchet mean on the manifold of symmetric positive definite (spd) matrices with log-euclidean metric. *arXiv preprint arXiv:2208.04245*, 2022. [12](#)

- [33] C. F. Van Loan and N. Pitsianis. Approximation with Kronecker products. In Marc S. Moonen, Gene H. Golub, and Bart L. R. De Moor, editors, *Linear Algebra for Large Scale and Real-Time Applications*, pages 293–314. Springer Netherlands, Dordrecht, 1993. 15
- [34] Ami Wiesel. On the convexity in Kronecker structured covariance estimation. In *2012 IEEE Statistical Signal Processing Workshop (SSP)*, pages 880–883. IEEE, 2012. 26